CHAPTER III

RESULTS

3.1 Characterization of Sll0337 and Slr0081 using oligonucleotide-directed mutagenesis

3.1.1 *Identification of the start codon of Sll0337*

Alignments of the amino acid sequences of Sll0337 and Slr0081 with those of PhoR of other cyanobacteria and *E. coli* indicated that the start codon of *sll0337* is different from the annotation in Cyanobase (http://www.kazusa.or.jp/cyano/cyano.html) whereas the start codon of *slr0081* appeared to be identified correctly. The start codon of *phoR* gene from the sequence alignment was ATG while that in Cyanobase was GTG. Thus, the annotation in cyanobase indicated that PhoR lacked 47 amino acids (Fig. 7). Therefore RT-PCR and 5'-RACE was carried out to identify the correct start codon of *sll0337*.

The RNA was extracted from the cell pellet grown in phosphate-limiting BG-11. The cDNA was achieved by reverse transcription by using sll0337 gene specific primer (primer 1). The poly A tail was added to the 3' end of the cDNA. The cDNA with the poly A tail was amplified using the primers sll0337 (reverse primer 1) and an oligo d(T)-anchor primer. The PCR reaction was used to amplify the DNA fragment using the PCR conditions as follows: an initial denaturation at 95°C for 4 min followed by 30 cycles consisting of 1 min annealing at 51°C, 1 min extension at 72°C and 30 s denaturing at 94°C. The reaction was ended with a final extension at 72°C for 5 min. A second round of PCR was performed using 5 μl of first round PCR

Figure 7 Nucleotide sequence of *sll0337*. Nucleotide sequence of *sll0337* from PhoR cyanobacterial sequence alignment (black letters) and Cyanobase (blue letters). The start codon of sll0337 from alignment and Cyanobase are indicated by red and black boxes, respectively. The stop codon of sll0337 is indicated in green box.

product, the sll0337 primer (reverse primer 2) and anchor primer. The PCR reaction involved an initial denaturation at 95°C for 4 min followed by 30 cycles consisting of 1 min annealing at 54°C, 1 min extension at 72°C and 30 s denaturing at 94°C. The reaction was ended with a final extension at 72°C for 5 min. The PCR product from the second round of PCR was checked on 0.8% agarose gel (Fig. 8).

The PCR product 0.65 kb band from second round of PCR (Fig. 8, lane 3) was cut, purified and cloned into the pGEMT-Easy vector. The plasmid was extracted and sequenced by using the universal primer. The result indicated that ATG, not GTG, was the start codon of *sll0337* in *Synechocystis* sp. PCC 6803 (Fig. 9)

3.1.2 *Construction of the PhoR and PhoB strains for mutagenesis*

To create specific amino acid *Synechocystis* sp. PCC 6803 mutant strains, the mutagenesis plasmid containing the specific mutations has to be transformed into the corresponding deletion strain. The mutagenesis plasmid was constructed by insertion of the antibiotic-resistance cassette downstream of the gene. This plasmid was named as the control plasmid. The deletion strain was constructed by transforming the deletion plasmid, which was constructed by replacing the ORF of gene with antibiotic-resistance cassette, into wild type *Synechocystis* sp. PCC 6803.

The mutagenesis plasmid, pTZsll0337-kan^R and Δsll0337-cam^R deletion strain that was used for the construction of mutants at Thr-214 of Sll0337 were obtained from laboratory stocks. The restriction enzyme digestion of pTZsll0337-kan^R and genomic PCR of Δ*sll0337*-cam^R strain were carried out to confirm that the desired plasmid and deletion strain had been obtained from the laboratory stocks.

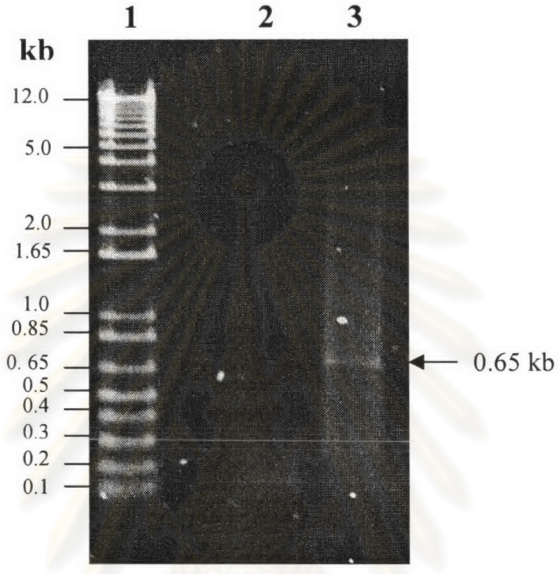

Figure 8 PCR product from 5'-RACE. PCR product was analysed on 0.8% agarose gel electrophoresis. 1 Kb Plus DNA marker (lane 1), negative control in which no reverse transcriptase adding (lane 2) and PCR product from 5'-RACE (lane 3).

TTTTTTTTTTTTTTTTTTGGAAAAAATGCTGCTCCGGACTAGG
CAACTGCTAGAACATGGAAATAATTACATTGGCGATCGGCGG
GGCAATTGGTTTTGGCATCGGGGCGATCGAACGGTTTCGGCT
CAATAATAAAATTAAAAAATTGCTCACTGGGCTGCCGGATAC
CCAGGAAGTTTCCCATTCCCTGTCCCTTGTGTCCCTGGTGCG
GCGAGAAATTAATCACTTAAATGATCTCTGTGCGGAATATCT
AGATACCATTGCCCATTGGCGGGGAGTAATGTCCCTTTCTCC
CC----------

Figure 9 Nucleotide sequence of PCR product from 5'-RACE. The translation start codon of *sll0337* of *Synechocystis* sp. PCC 6803 is indicated in blue letters. The translation start codon from cyanobase is shown in red letters.

The *EcoR* I digest yielded fragment of 4.1 kb and 1.9 kb and the *Hind* III digest resulted in three bands of 4.0 kb, 1.4 kb and 0.6 kb (Fig. 10). These restriction digests confirmed that the pTZsll0337-kan^R plasmid was correct.

The PCR products from wild type and the Δsll0337-cam^R mutant were expected to be 2.2 kb and 3.6 kb, respectively. The PCR reaction involved an initial denaturation at 95°C for 4 min followed by 30 cycles consisting of 1 min annealing at 62°C, 3 min extension at 72°C and 30 s denaturing at 94°C. The reaction was ended with a final extension at 72°C for 5 min. The PCR products obtained conform to the predicted sizes (Fig. 11) therefore, the Δsll0337-cam^R mutant was the correct strain.

The mutagenesis plasmid, pTZslr0081-cam^R and the Δslr0081-spec^R deletion strain required for making mutation at Asp-88 of Slr0081 were obtained from laboratory stocks. The restriction enzyme digestion of the pTZslr0081-cam^R plasmid and genomic PCR of the Δslr0081-spec^R strain were carried out to confirm that there were the desired plasmid and strain.

The *EcoR* I digest yielded fragments of 4.8 kb and 2.8 kb and the *Hind* III digest resulted in two bands of 6.6 kb and 0.9 kb (Fig. 12). These restriction digests confirmed that the pTZslr0081-cam^R plasmid was correct.

The PCR products from wild type and the Δslr0081-spec^R strain were expected to be 2.6 kb and 1.9 kb, respectively. The PCR products obtained conformed to the predicted sizes (Fig. 13) therefore, the Δslr0081-spec^R was the correct strain.

However, in previous studies the control plasmids of both *sll0337* and *slr0081* had not been transformed into wild type *Synechocystis* sp. PCC 6803 for construction of control strains. In this study, these strains were made to ascertain that the antibiotic

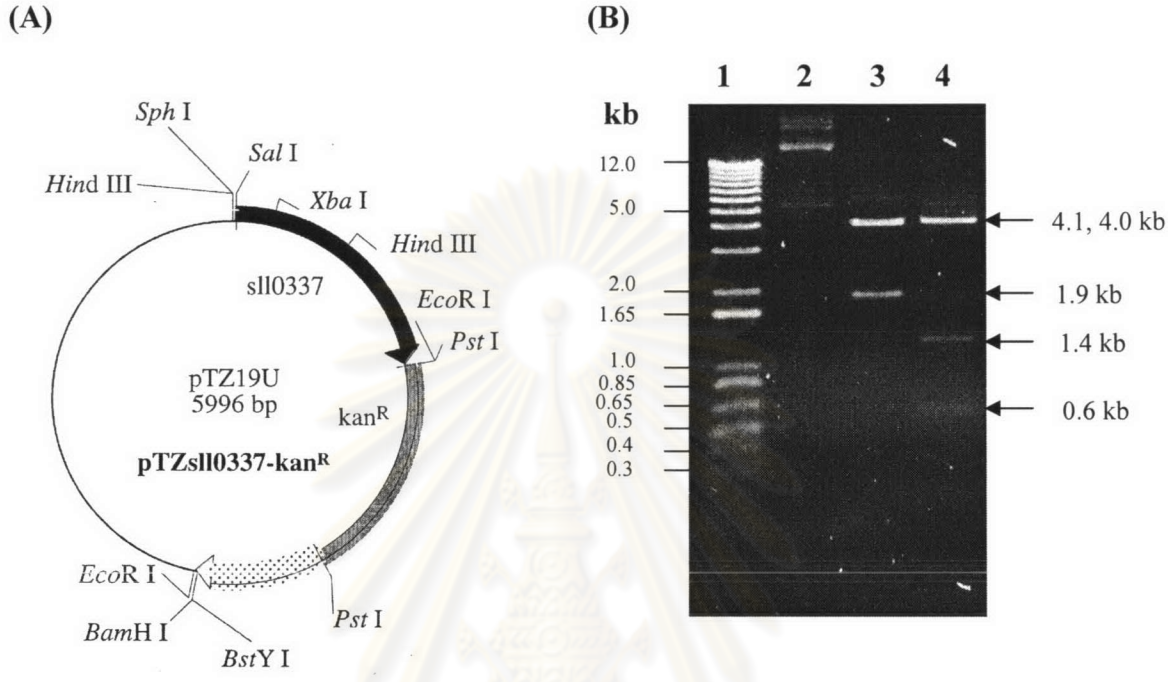

Figure 10 The pTZsll0337-kan^R plasmid. (A) The *sll0337* gene was cloned into pTZ19U. The kanamycin-resistance cassette is inserted at the *Pst* I site located downstream of the *sll0337* gene. The *sll0337* gene and kanamycin-resistance cassette are showed by black and gray arrows, respectively. (B) Restriction enzyme digests of pTZsll0337-kan^R. Digested plasmids were analysed on 0.8% agarose gel electrophoresis. 1 Kb Plus DNA marker (lane 1), uncut plasmid (lane 2), *EcoR* I digest (lane 3) and *Hind* III digest (lane 4).

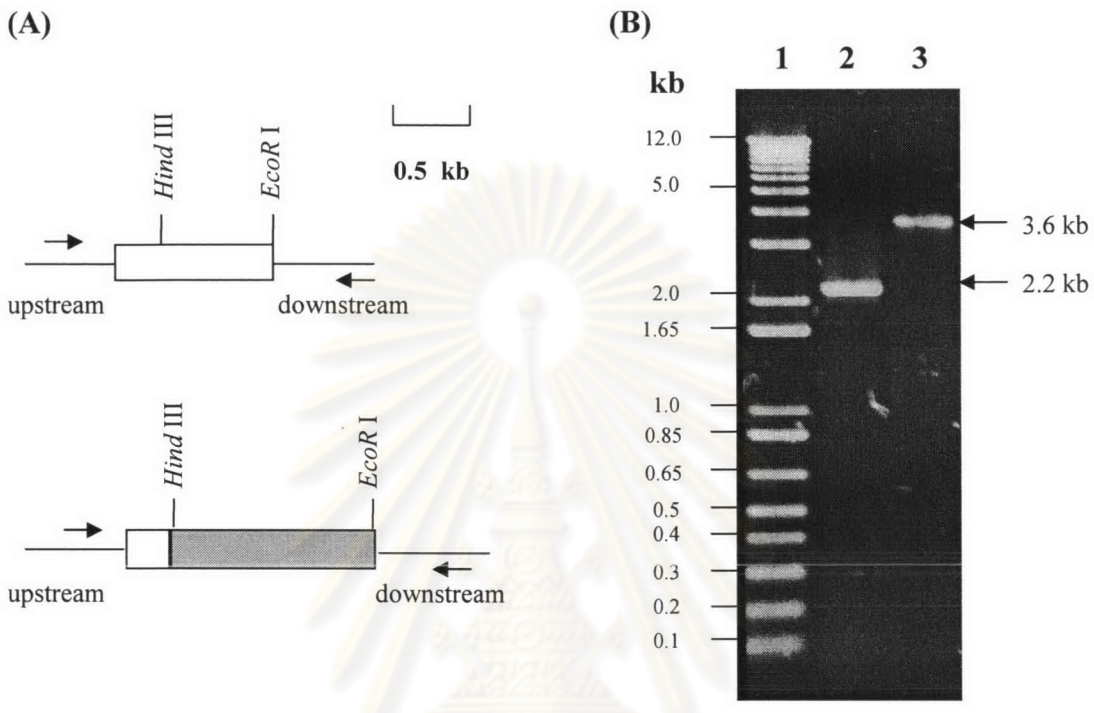

Figure 11 PCR demonstrating Δsll0337-cam^R strain. (A) DNA map showing the *sll0337* gene and Δsll0337-cam^R. The chloramphenicol-resistance cassette is inserted at the *EcoR* I and *Hind* III site. The *sll0337* and chloramphenicol-resistance cassette are shown by white and gray boxes, respectively. The *sll0337* forward and reverse primers are shown by arrows. (B) PCR products were analysed on 0.8% agarose gel electrophoresis. 1 Kb Plus DNA marker (lane 1), wild type (lane 2) and Δsll0337-cam^R strain (lane 3).

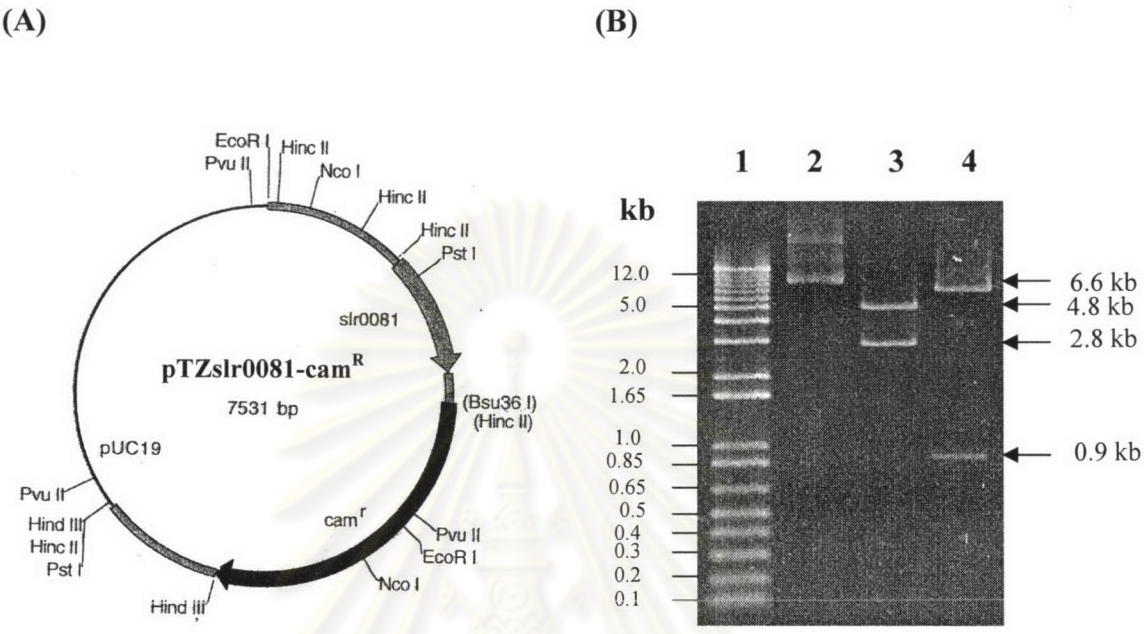

Figure 12 The pTZslr0081-cam^R plasmid. (A) The *slr0081* gene was cloned into pTZ19U. The chloramphenicol-resistance cassette was inserted at the *Bsu*36 I site downstream of *slr0081* gene. The *slr0081* and chloramphenicol-resistance cassette are shown by gray and black arrows, respectively. (B) Restriction enzyme digests of pTZslr0081-cam^R were analysed on 0.8% agarose gel electrophoresis. 1 Kb Plus DNA marker (lane 1), uncut plasmid (lane 2), *EcoR* I digest (lane 3) and *Hind* III digest (lane 4).

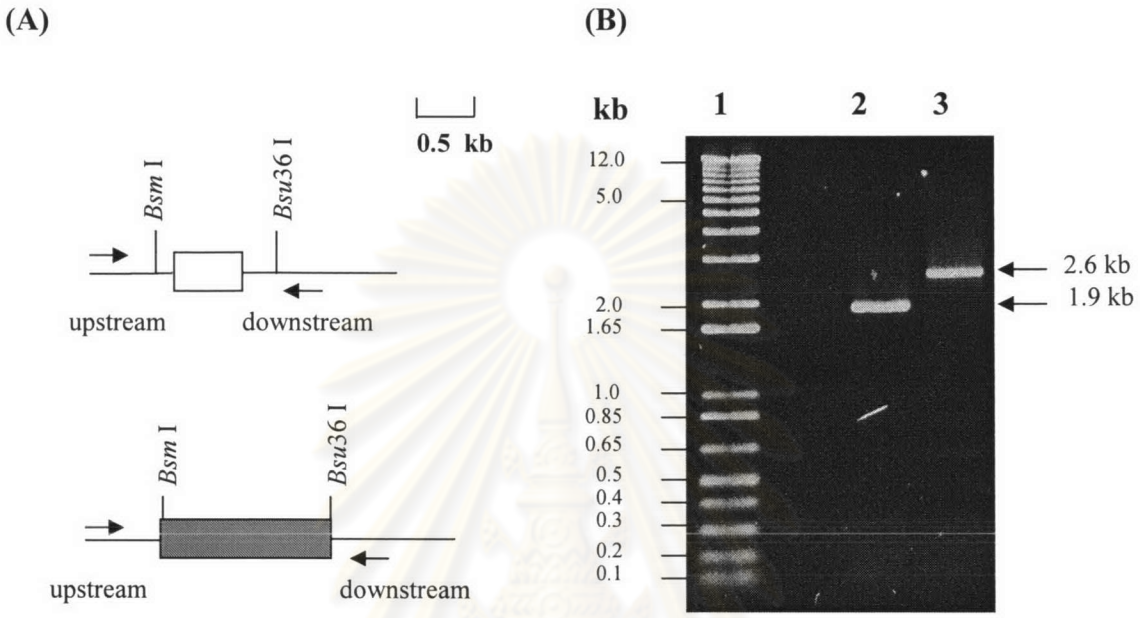

Figure 13 PCR from genomic DNA obtained from the Δslr0081-spec^R strain on 0.8% agarose gel electrophoresis. (A) Genomic map showing the slr0081 gene in wild type and the Δslr0081-spec^R mutant. The spectinomycin-resistance cassette was inserted at the *Bsm* I and *Bsu*36 I sites. The *slr0081* and spectinomycin-resistance cassette are shown by white and gray boxes, respectively. The slr0081 forward and reverse primers are shown by arrows. (B) PCR products were analysed on 0.8% agarose gel electrophoresis. 1 Kb Plus DNA marker (lane 1), wild type (lane 2) and Δslr0081-spec^R (lane 3).

cassette, included in the mutagenesis plasmid construct as a selectable marker, had no unexpected deleterious effect in the resulting strains. The photoautotrophic growth was followed in both deletion and control strains comparing to wild type under normal BG-11 and phosphate-limiting conditions.

After the wild type of *Synechocystis* sp. PCC 6803 was transformed with the sll0337 control plasmid, the homozygosity of the strains was verified by southern blot analysis comparing between wild type and the Δsll0337 strain. In this experiment, the genomic DNA was digested with *Dra* I. The expected 3.5 kb, 2.4 kb and 2.3 kb bands were obtained from the wild type, control and deletion strains, respectively. To determine whether the deletion and control strains could grow under phosphate-limiting conditions as well as in normal BG-11, their photoautotrophic growth was compared to that of wild type. All strains exhibited similar growth in both conditions (Fig. 14).

When the same experiment was conducted in the Slr0081 strain. The genomic DNA was digested with *Ava* I and *EcoR* I. The expected 3.8 kb, 3.2 kb and 1.1 kb bands were obtained in the wild type, control and deletion strains, respectively. Similarly, no difference in the growth among these three strains was observed (Fig. 15).

After the results showed that the antibiotic-resistance cassette had no effect on the phenotype of the mutant strains, the mutations at Thr-214 of Sll0337 and Asp-88 of Slr0081 were constructed by using oligonucleotide-directed mutagenesis. The mutants and wild type cells were grown in normal and phosphate-limiting BG-11 for 24 hours. The effects of these mutations were determined by measuring the alkaline phosphatase activity, *in vivo*.

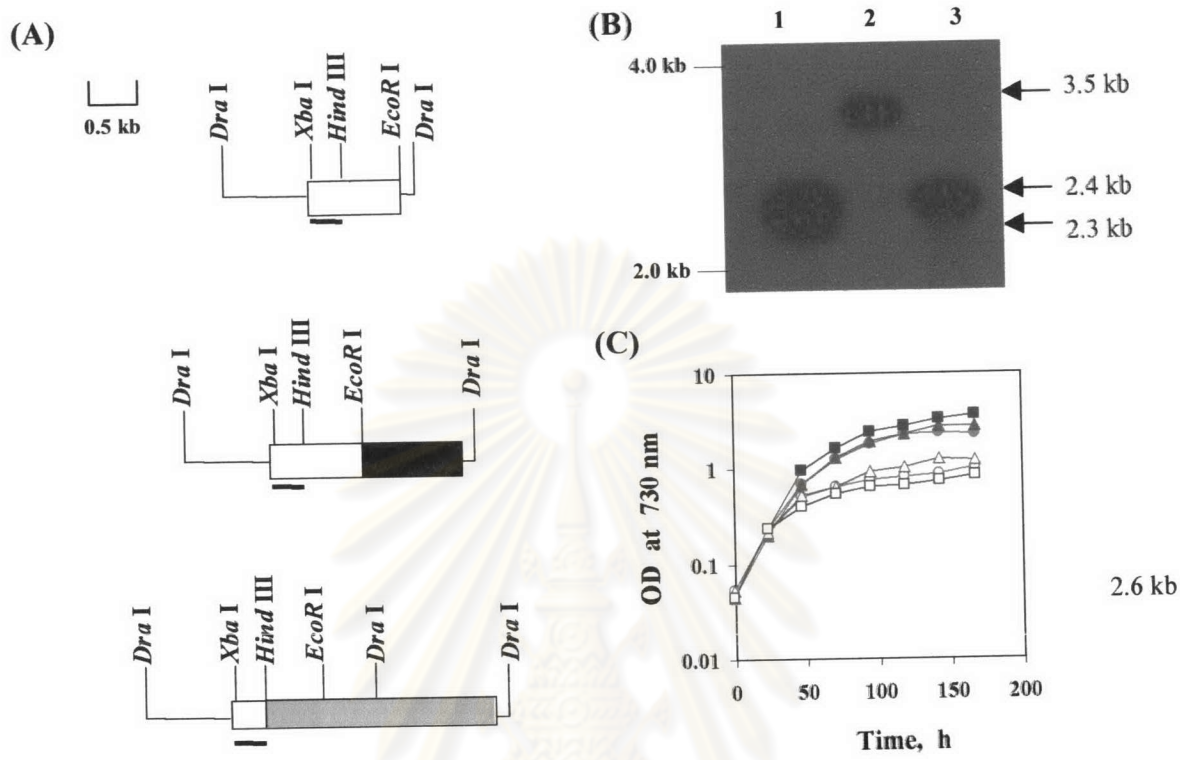

Figure 14 Confirmation of the Sll0337 mutants and their photoautotrophic growth. (A) Restriction map of the *sll0337* region of genomic DNA showing the wild type (top), PhoR:control (middle) and ΔPhoR (bottom). The *sll0337*gene, kanamycin-resistance cassette and chloramphenicol-resistance cassette are shown by open, black and grey boxes, respectively. (B) Southern blot of wild type (lane 1), Sll0337:control (lane 2) and ΔSll0337 (lane 3). Genomic DNA was digested with *Dra* I and probed using a 404 bp *Xba* I/*Hind* III DNA fragment indicated by a bold line in (A). (C) Photoautotrophic growth of strains as measured by the optical density at 730 nm in normal BG-11 (closed symbols) and in phosphate-limiting BG-11 (open symbols). Wild type (red), sll0337:control (blue) and Δsll0337 (green).

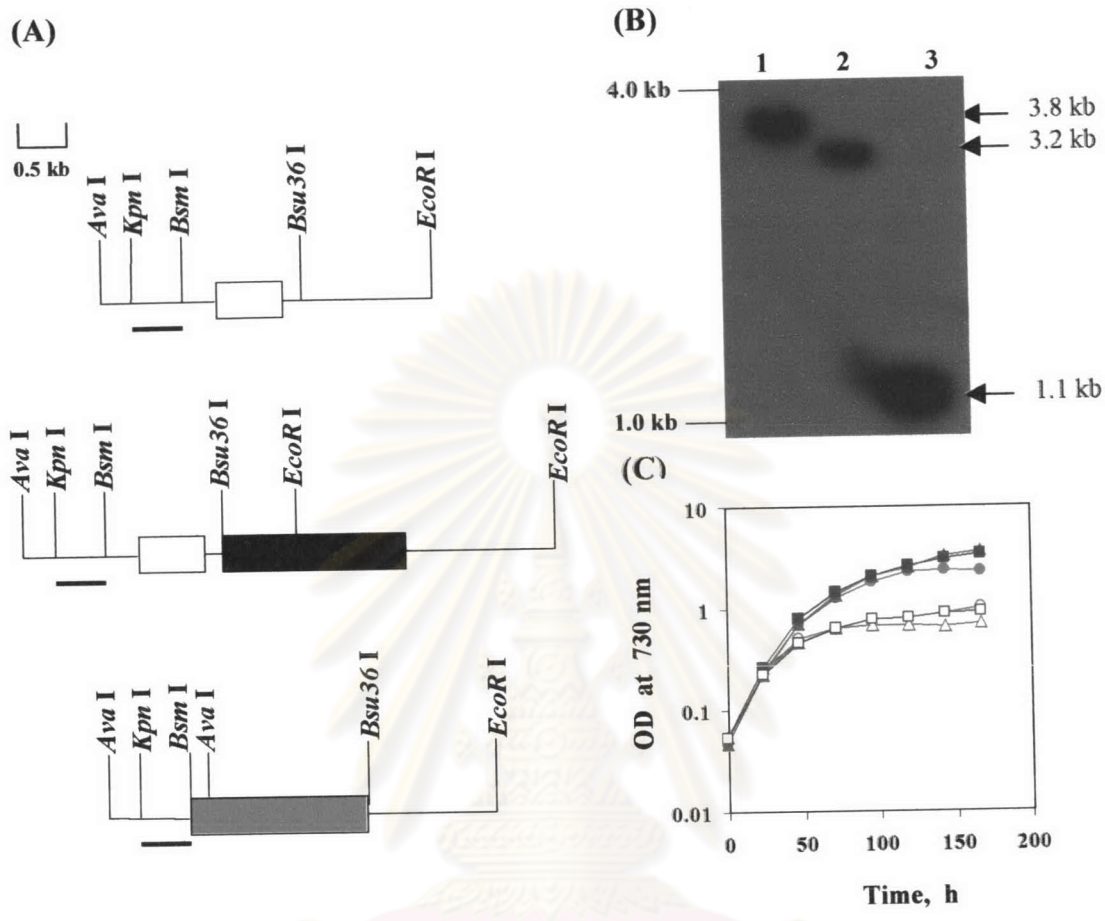

Figure 15 Confirmation of the Slr0081 mutants and their photoautotrophic growth. (A) Restriction map of the *slr0081* region of genomic DNA showing the wild type (top), slr0081:control (middle) and Δslr0081 (bottom). The slr0081 gene, chloramphenicol-resistance cassette and spectinomycin-resistance cassette are shown by open, black and gray boxes, respectively. (B) Southern blot of wild type (lane 1), slr0081:control (lane 2) and Δslr0081 (lane 3). Genomic DNA was digested with *Ava* I and *EcoR* I and probed using a 580 bp *Kpn* I/*Bsm* I DNA fragment indicated by the bold line in (A). (C) Photoautotrophic growth of strains as measured by the optical density at 730 nm in normal BG-11 (closed symbols) and in phosphate-limiting BG-11 (open symbols). Wild type (red), slr0081:control (blue) and Δslr0081 (green).

3.1.3 *Thr-214 mutation involved in the regulation of alkaline phosphatase activity*

Since the histidine kinase from *E. coli* contains both polar and nonpolar residues at position 214 such as Ser, Thr, Asn, Ala and Gly. Previously, the substitution of Thr-214 with Asn was constructed (Simpson, 2003). The result showed the constitutive induction of alkaline phosphatase activity. However, the activity in the phosphate-sufficient condition did not reach the level of activity in phosphate-limiting condition. Therefore, the Thr-214 was further mutated to Ser, Ala, Arg, Gln and Gly in this study.

After these specific mutagenesis plasmids were constructed, they were transformed to the Δsll0337 strain. The mutant strains were streaked on the antibiotic selection plates. The homozygosity of these strains was verified by PCR reaction using the sll0337 forward and reverse primers. The PCR reaction involved an initial denaturation at 95°C for 4 min followed by 30 cycles consisting of 1 min annealing at 62°C, 1 min extension at 72°C and 30 s denaturing at 94°C. The reaction was ended with a final extension at 72°C for 5 min.

It can be seen that the genomic DNA of Thr-214 mutants possessed the expected single band at 3.4 kb while single bands of 3.6 kb and 2.2 kb was obtained from Δsll0337 and wild type, respectively. The difference in size of single PCR product in each lane indicated that the introduced copy of sll0337 had fully segregated sll0337:control strain (Fig. 16). Hence these Thr-214 mutants including the T214N strain were used for the study of the effect of the specific mutations on alkaline phosphatase activity under normal and phosphate-limiting conditions.

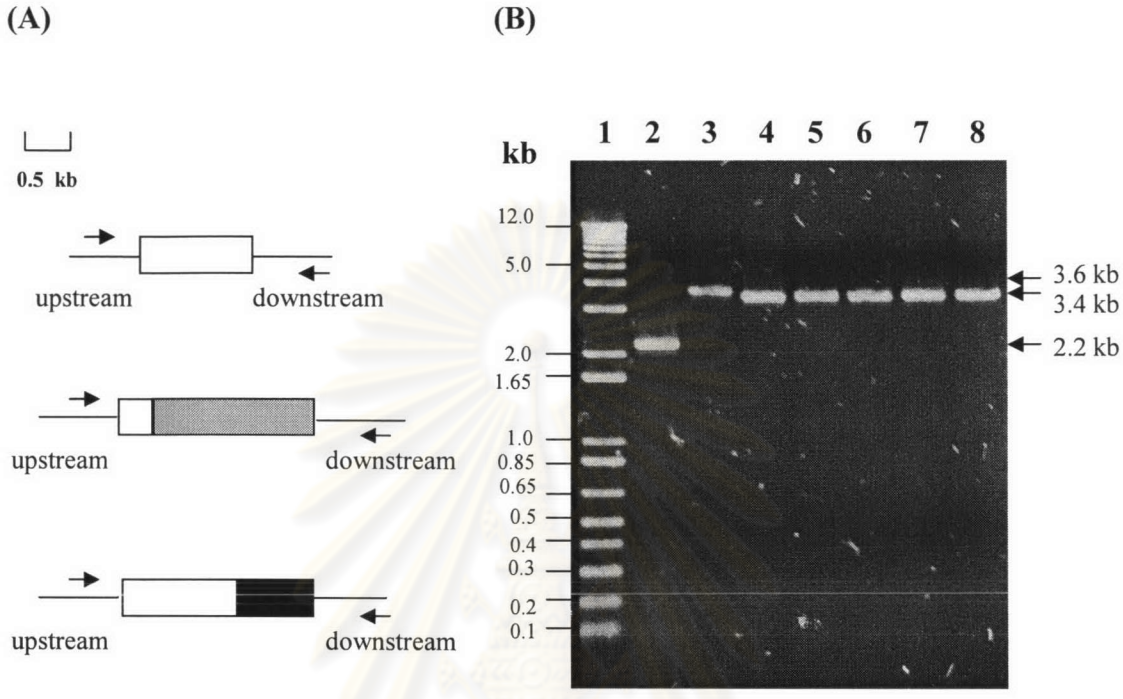

Figure 16 PCR demonstrating full segregation of the introduced sll0337 in the control and Thr mutant strains. (A) Genomic map showing the sll0337 region in wild type, Δ*sll0337* and *sll0337*-kan^R strains. The *sll0337*, chloramphenicol and kanamycin-resistance cassette are shown by white, gray and black boxes, respectively. The sll0337 forward and reverse primers are shown by arrows. (B) PCR products were analysed on 0.8% agarose gel electrophoresis. 1 Kb Plus DNA marker (lane 1), wild type (lane 2), Δsll0337 (lane 3), T214S (lane 4), T214A (lane 5), T214R (lane 6), T214Q (lane 7) and T214G (lane 8).

When Thr-214 was substituted with Ser, Ala, Gln, Gly and Asn, alkaline phosphatase activity for all mutants grown for 1 day could be induced in both normal BG-11 and phosphate-limiting conditions (Fig. 17, lanes 2-6). However, this was not the case for T214R (Fig. 17, lane 7). The whole-cell spectra of 1 day and 4 days T214R cells are shown in Fig. 18. The absorption maxima at 680 nm and 440 nm, due to chlorophyll *a* and the peak at 620 nm, corresponding to phycobilins, are significantly reduced when phosphate was omitted from the growth medium. The results suggested that under phosphate-limiting condition, a 4- day stress was more severe than a 1- day stress. However, at 4 days phosphate stress the induction of alkaline phosphatase was still undetectable (data not shown). It can be inferred that all amino acids tested except the positively charged residue could be located at position 214.

For the Asn, Ser, Ala, Gln and Gly substitution, the resulting mutant exhibited an unusual and interesting phenotype under phosphate-sufficient condition (Fig. 17, lanes 2-6). The repression of the *pho* regulon was not as effective as seen in wild type. Since PhoU may interact with the Pst system or PhoR to form the repression complex, double mutants were constructed. Double mutants were constructed combining with the original histidine kinase mutations with the interruption of the *phoU* gene to investigate whether Thr-214 interacts with PhoU.

3.1.4 *The effect of the removal of PhoU from the Thr-214 mutants*

The *phoU* deletion strain had been constructed by Simpson (2003). The *phoU* gene was interrupted with chloramphenicol-resistance cassette to determine the involvement of the PhoU protein in the repression of the *pho* regulon. The pΔphoU

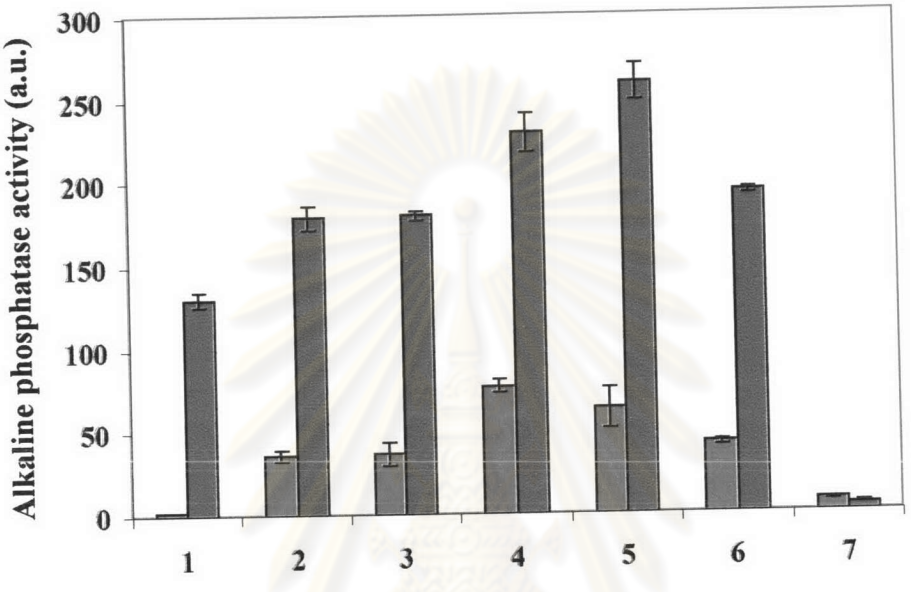

Figure 17 Measurement of alkaline phosphatase activity in strains carrying mutations at Thr-214 in Sll0337 under phosphate-sufficient and phosphate-limiting conditions. Cells were grown in normal BG-11 (blue bars) and in phosphate-limiting BG-11 (purple bars). The strains are wild type (1), T214N (2), T214S (3), T214A (4), T214Q (5), T214G (6) and T214R (7). The data represent Mean $\pm$ SD, n=3.

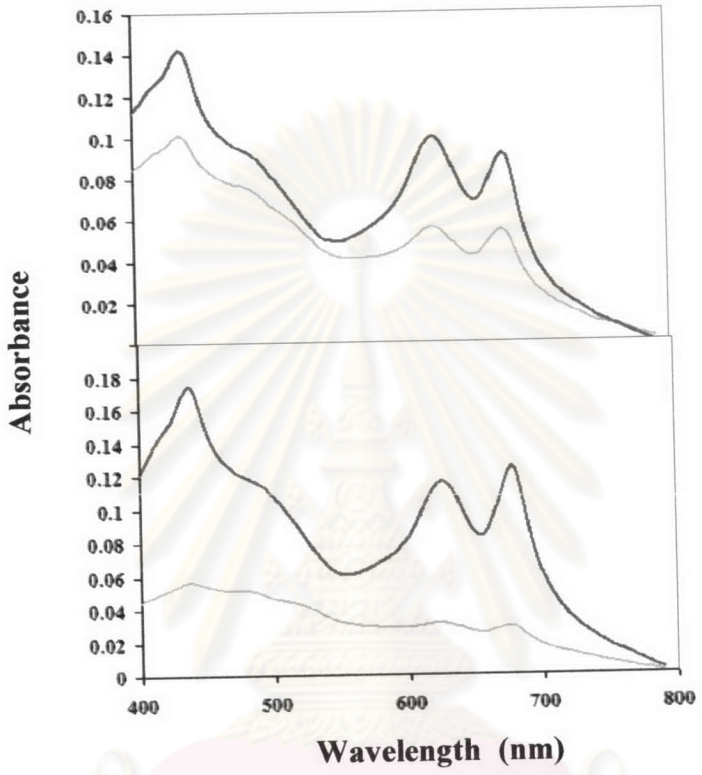

Figure 18 Whole-cell absorption spectrum of wild type and T214R under phosphate-sufficient (green) and phosphate-limiting conditions (orange) grown for 1 day (top) and 4 days (bottom).

construct obtained from laboratory stocks was checked by restriction enzyme digestion before transforming into Thr-214 mutants.

The *Nco* I digest yielded fragments of 3.0 kb, 1.6 kb, 1.1 kb and 0.9 kb. The *Not* I digest resulted in two bands of 3.8 kb and 2.9 kb and *Cla* I was expected to linearise the plasmid, resulting in a 6.8 kb band (Fig. 19). These restriction digests comfirmed that the pΔPhoU plasmid was correct.

The pΔphoU plasmid was transformed into the Thr-214 mutants. The resulting mutant strains were streaked on the antibiotic selection plates and homozygosity of these strains was verified by PCR using the slr0741 forward and reverse primers. The PCR reaction involved an initial denaturation at 95°C for 4 min followed by 30 cycles consisting of 1 min annealing at 62°C, 1 min extension at 72°C and 30 s denaturing at 94°C. The reaction was ended with a final extension at 72°C for 5 min.

The result from Fig. 20 exhibited that the genomic DNA of Thr-214:ΔPhoU results in a single clean band of 3.9 kb while the wild type strain gave the 1.8 kb band. Therefore these mutant strains had fully segregated and expressed the 2 kb chloramphenicol-resistance cassette in all copies of the genome. The effect of mutation in these strains including Thr-214N:ΔPhoU, which was constructed by Simpson (2003), was determined by measuring the induction of alkaline phosphatase activity.

The wild type showed low alkaline phosphatase activity under phosphate-sufficient condition (Fig. 21, lane 1), the ΔPhoU showed much higher alkaline phosphatase activity which was similarly induced in both phosphate-sufficient and phosphate-limiting conditons (Fig. 21, lane 2), suggesting the role of PhoU as a

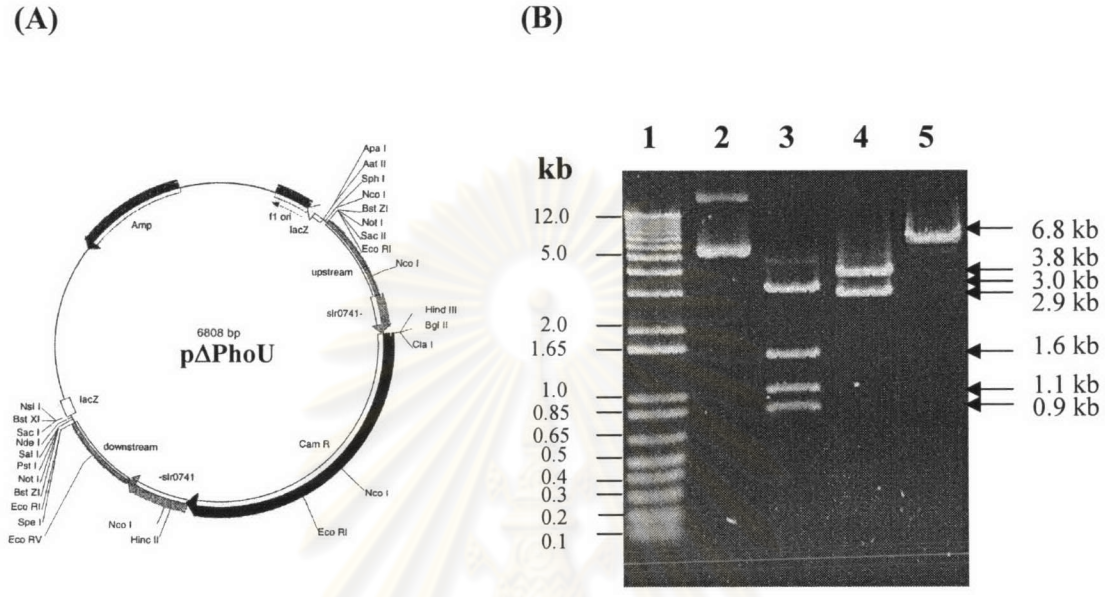

Figure 19 The pΔPhoU mutant plasmid. (A) The chloramphenicol-resistance cassette was inserted to the pPhoU plasmid. The *slr0741* gene and chloramphenicol-resistance cassette are shown by black and gray arrows, respectively. (B) Restriction enzyme digests of the pΔPhoU plasmid were analysed on 0.8% agarose gel electrophoresis. 1 Kb Plus DNA marker (lane 1), uncut plasmid (lane 2), *Nco* I digest (lane 3), *Not* I digest (lane 4) and *Cla* I digest (lane 5).

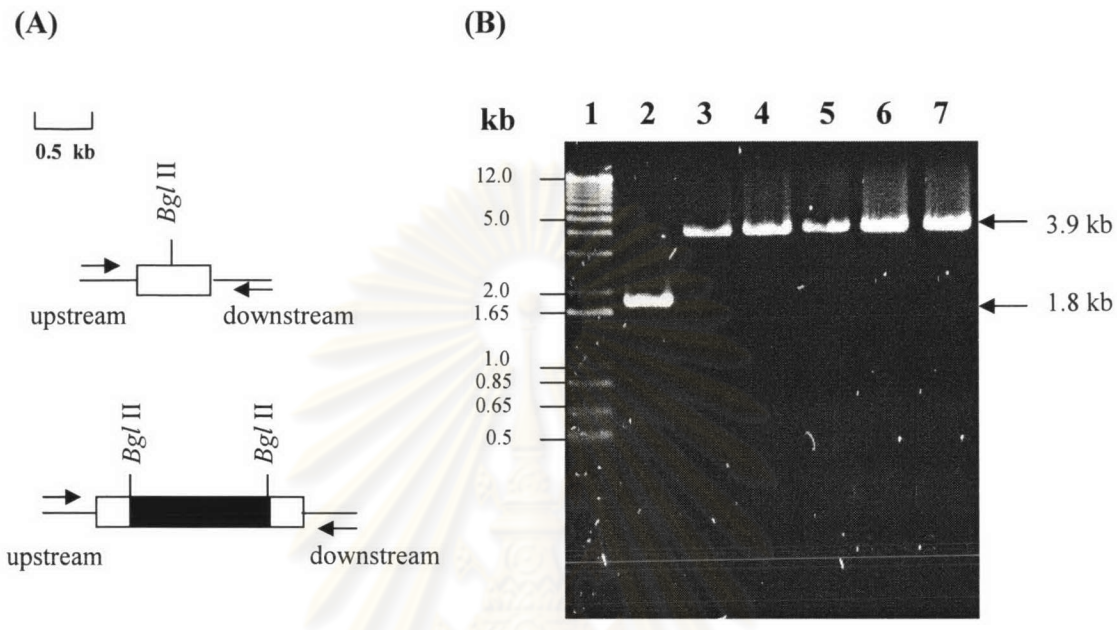

Figure 20 PCR demonstrating full segregation of the gene encoding the interrupted copy of phoU in the histidine kinase mutants. (A) Genomic map showing the *phoU* gene and the presence of the chloramphenicol-resistance cassette in the inactivated gene at *Bgl* II site. The *phoU* gene and chloramphenicol-resistance cassette are shown by white and black boxes, respectively. The slr0741 forward and reverse primers are shown by arrows. (B) PCR products were analysed on 0.8% agarose gel electrophoresis. 1 Kb Plus DNA marker (lane 1), wild type (lane 2), T214S:ΔPhoU (lane 3), T214A:ΔPhoU (lane 4), T214R:ΔPhoU (lane 5), T214Q:ΔPhoU (lane 6) and T214G:ΔPhoU (lane 7).

negative regulator of alkaline phosphatase. Similar results were obtained in other ΔPhoU-histidine kinase double mutant strains (Fig. 21, lane 3-6) except for the T214N:ΔPhoU (Fig. 21, lane 7) and T214R:ΔPhoU (Fig. 21, lane 8) strains which showed little and no activity, respectively. These results suggested a possible interaction between Thr-214 and PhoU because if there were no interaction between these proteins, the alkaline phosphatase activity in the double mutant strains should have been similar to that of ΔPhoU strain. Interestingly, the T214R:ΔPhoU abolished the induction of alkaline phosphatase (Fig. 21, lane 8). This lent support for the importance of Thr-214 as for the function of PhoR. The whole-cell spectra of T214R:ΔPhoU cells grown under phosphate-limiting conditions for 1 day and 4 days are shown in Fig. 22. The absorption maxima at 680 nm and 440 nm, due to chlorophyll *a* and the peak at 620 nm, corresponding to phycobilins, are significantly reduced when phosphate was omitted from the growth medium. The results suggested that under phosphate-limiting condition, a 4- day stress was more severe than a 1- day stress; however, after the 4- day stress the induction of alkaline phosphatase was still undetectable (data not shown).

3.1.5 *Mutation Asp-88 in the receiver domain of Slr0081*

When the Slr0081 amino acid sequences were aligned with PhoB of other cyanobacteria and *E. coli*, the results indicated that Asp-88 was the site of phosphorylation in *Synechocystis* sp. PCC 6803. Thus, the Asp-88 was substituted by Asn.

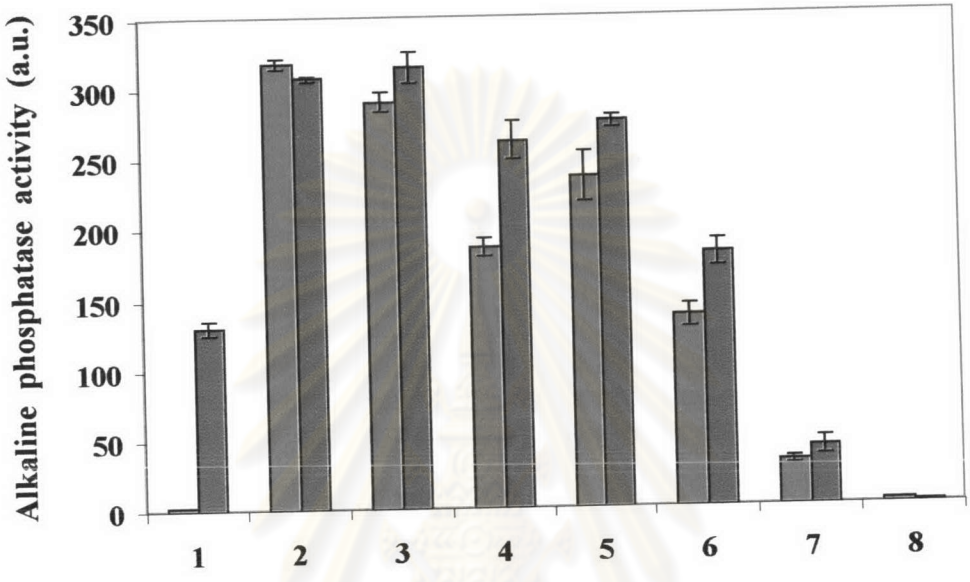

Figure 21 Measurement of alkaline phosphatase activity in strains carrying mutations at Thr-214 in the absence of PhoU under phosphate-sufficient and phosphate-limiting conditions. Cells were grown in normal BG-11 (blue bars) and in phosphate-limiting BG-11 (purple bars). The strains are wild type (1), ΔPhoU (2), T214S:ΔPhoU (3), T214A:ΔPhoU (4), T214Q:ΔPhoU (5), T214G:ΔPhoU (6), T214N:ΔPhoU (7) and T214R:ΔPhoU (8). The data represent Mean ± SD, n=3.

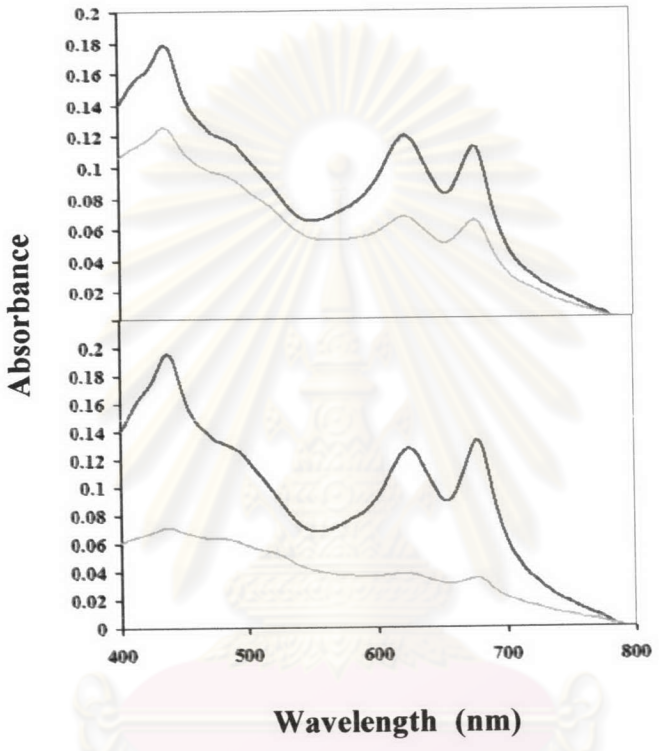

Figure 22 Whole-cell absorption spectrum of wild type and T214R:ΔPhoU under phosphate-sufficient (green) and phosphate-limiting conditions (orange) grown for 1 day (top) and 4 days (bottom).

After a specific mutagenesis plasmid was constructed, it was transformed to the Δslr0081 strain. The mutant strain was streaked on antibiotic selection plates. The homozygosity of this strain was verified by PCR using the slr0081 forward and reverse primers (Fig. 23). The PCR reaction involved an initial denaturation at 95°C for 4 min followed by 30 cycles consisting of 1 min annealing at 59°C, 3 min extension at 72°C and 30 s denaturing at 94°C. The reaction was ended with a final extension at 72°C for 5 min.

It can be seen that the genomic DNA of the Asp-88 mutant provides a single band of 4.1 kb while a single band of 2.6 kb and 1.9 kb was obtained from the Δslr0081 stain and wild type, respectively (Fig. 23). The difference in size of the PCR product in each lane indicated that the introduced copy of slr0081 in the control strain, together with the chloramphenicol-resistance marker, had fully segregated in slr0081: control strain. Therefore the D88N mutant was used for the study of the effect of this specific mutation on alkaline phosphatase activity under normal and phosphate-limiting conditions.

The results showed no induction of alkaline phosphatase activity when Asp was substituted with Asn (Fig. 24). Moreover, the whole-cell spectra following growth in phosphate-limiting conditions of 1- day and 4- days showed that under phosphate-limiting condition, the D88N cells were more severely stressed than a 1 day stress (Fig. 25). However, at even after 4 days under phosphate-limiting conditions the induction of alkaline phosphatase was still undetectable (data not shown). Overall these results indicated, therefore, that the aspartic acid at position 88 is the site of phosphorylation of Slr0081.

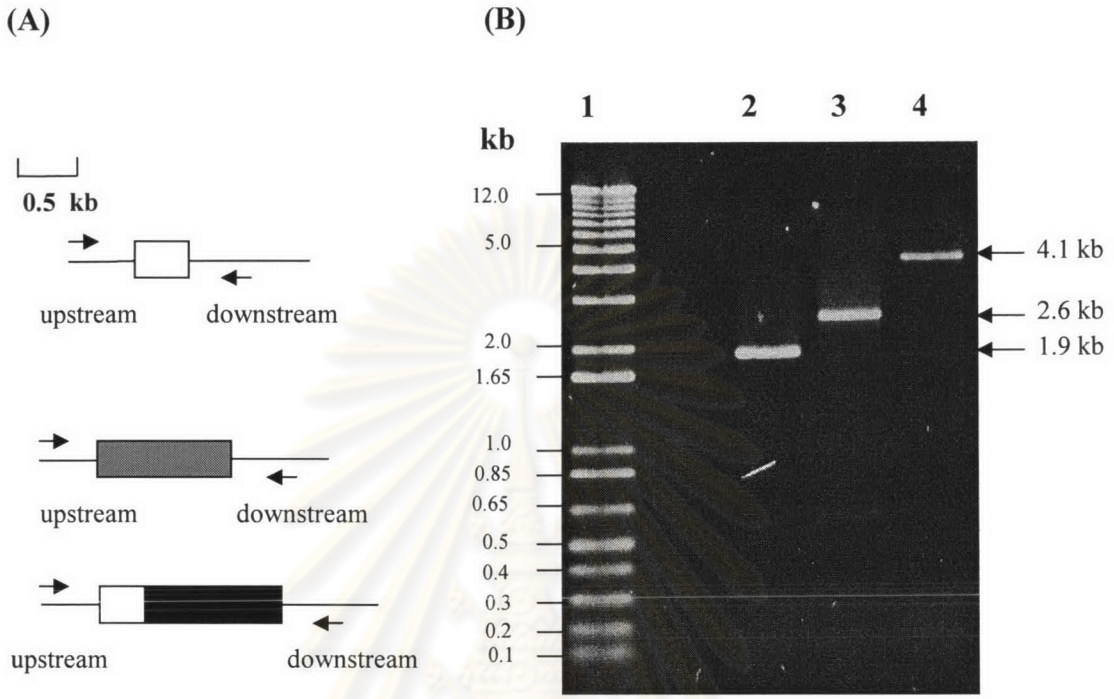

Figure 23 PCR demonstrating full segregation of slr0081:control. (A) Genomic DNA map showing the region of the *slr0081* gene. The slr0081 gene is shown by an open box and the spectinomycin-resistance cassette and chloramphenicol-resistance cassette are shown by gray and black boxes, respectively. PCR primers are shown by arrows. (B) 1 Kb Plus DNA marker (lane 1), wild type (lane 2), Δslr0081 (lane 3) and D88N (lane 4)

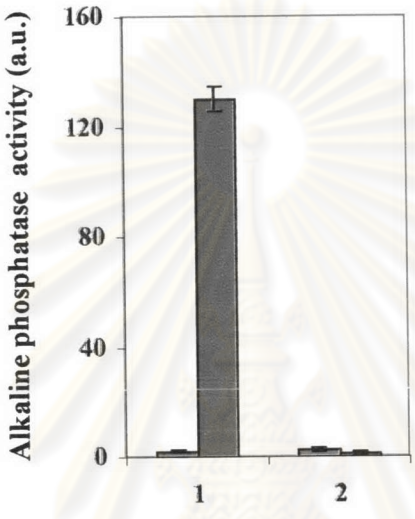

Figure 24 Measurement of alkaline phosphatase activity in the wild type and D88N strains under normal and phosphate-limiting conditions. Cells were grown in normal BG-11 (blue bars) and in phosphate-limiting BG-11 (purple bars). The strains are wild type (1), D88N (2). The data represent Mean $\pm$ SD, n=3.

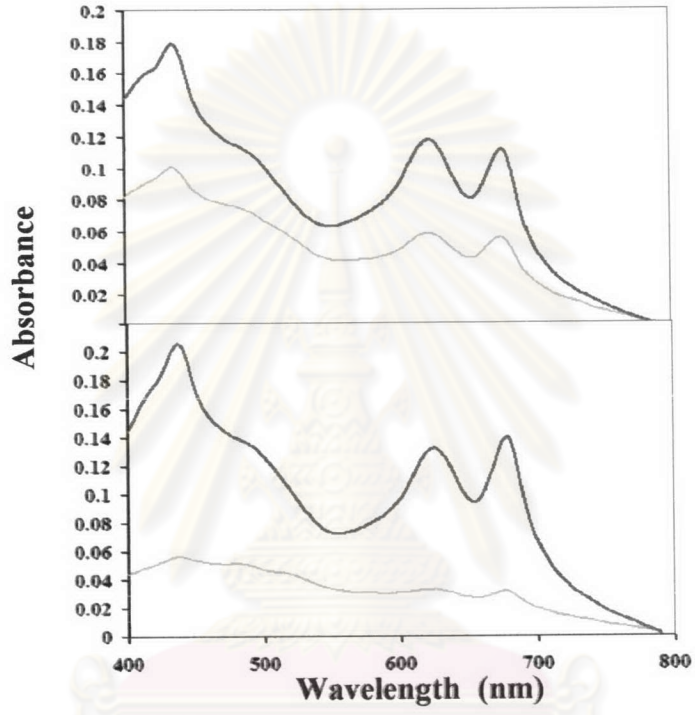

Figure 25 Whole-cell absorption spectrum of wild type and D88N under phosphate-sufficient (green) and phosphate-limiting conditions (orange) grown for 1 day (top) and 4 days (bottom).

There is no report about the possible interaction between PhoU and the response regulator protein. Therefore, the D88N strain lacking PhoU was studied. Since the selectable marker of the D88N mutant is the chloramphenicol-resistance cassette, the PhoU interruption with the same antibiotic cartridge plasmid, which was constructed by Simpsons (2003), cannot be used to construct the D88N:ΔPhoU mutant. Therefore a PhoU interruption mutant using a different antibiotic-resistance cassette was constructed in this study.

3.1.6 *Construction of the phoU interruption plasmid*

The pGEMT-easy plasmid containing the cloned *phoU* gene was interrupted with a kanamycin-resistance cassette. The position of *Bgl* II site was used for the insertion of the kanamycin-resistance cassette. This pΔphoU2 plasmid was confirmed by restriction enzyme digestion.

The *Sph* I digest was expected to linearise the plasmid, resulting in a 6.0 kb band and the *EcoR* I/*Cla* I digest yielded fragments of 3.0 kb, 1.8 kb and 1.2 kb (Fig. 26). The plasmid obtained conforms to the predicted sizes of each restriction digest thereby confirming the pΔPhoU2 containing a kanamycin-resistance cassette had been constructed.

This pΔphoU2 plasmid was transformed into the D88N mutant. The D88N:ΔphoU mutant strain was streaked on antibiotic selection plates. The homozygosity of this strain was verified by PCR using the slr0741 forward and reverse primers.

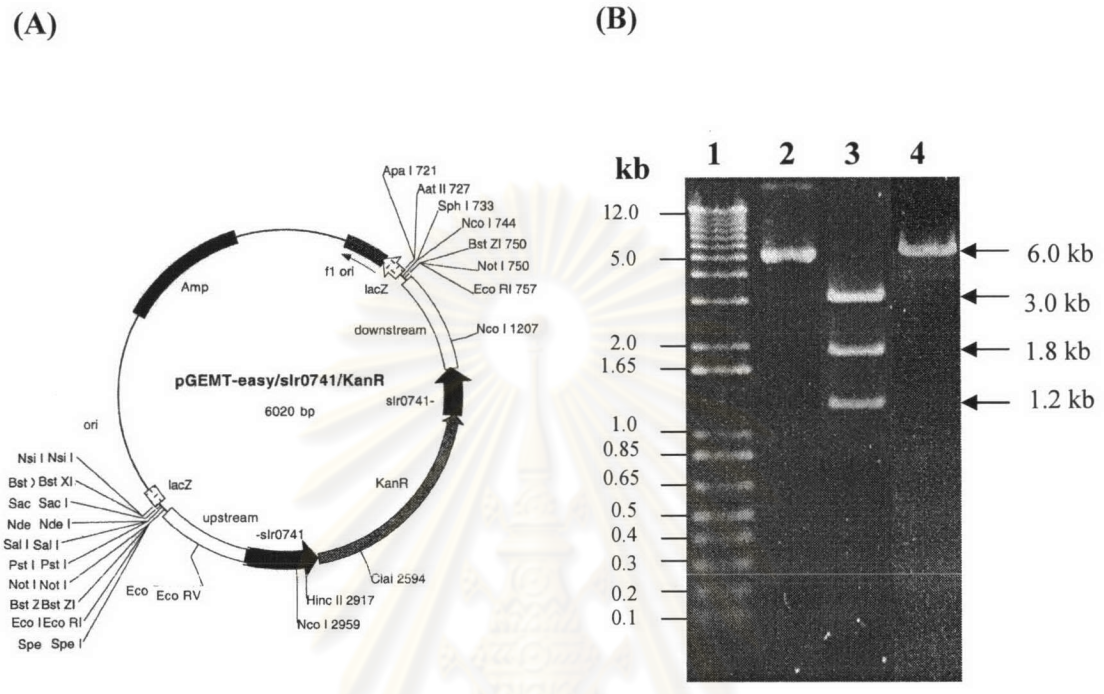

Figure 26 The pΔPhoU2 mutant plasmid. (A) The kanamycin-resistance cassette was inserted into the pPhoU plasmid at *Bgl* II site. The *slr0741* gene and kanamycin-resistance cassette are showed by black and gray arrows, respectively. (B) Restriction enzyme digests of the ΔPhoU2 construct were analysed on 0.8% agarose gel electrophoresis. 1 Kb Plus DNA marker (lane 1), uncut plasmid (lane 2), *EcoR I*/*Cla* I digest (lane 2) and *Sph* I digest (lane 3).

The PCR reaction involved an initial denaturation at 95°C for 4 min followed by 30 cycles consisting of 1 min annealing at 62°C, 1 min extension at 72°C and 30 s denaturing at 94°C. The reaction was ended with a final extension at 72°C for 5 min.

The result from Fig. 27 demonstrated that the genomic DNA of D88N:ΔPhoU resulted in a single band of 3.3 kb while the wild-type strain gave a 1.7 kb band. Therefore the mutant strains had fully segregated and expressed the 1.2 kb kanamycin-resistance cassette in all copies of the genome. Alkaline phosphatase activity was then investigated in the D88N:ΔPhoU cells under phosphate-limiting and phosphate-sufficient conditions (Fig. 28).

The wild type showed low alkaline phosphatase activity under phosphate-sufficient condition (Fig. 28, lane 1), the ΔPhoU showed much higher alkaline phosphatase activity (Fig. 28, lane 2). D88N:ΔPhoU showed no activity (Fig. 28, lane 3). This result demonstrates that the repression by PhoU can only be overcome if phosphotransfer to PhoB can occur.

3.1.7 *Dilution effect on alkaline phosphatase assay*

The assay for alkaline phosphatase in the Material and Methods chapter makes use of a chromogenic substrate called p-nitrophenyl phosphate (pNPP). Chromogenic means that the reaction gives color when products are created. The enzyme catalyzes the hydrolysis of the substrate to release inorganic phosphate and p-nitrophenol (Fig. 29).

The product, p-nitrophenol, is colorless when protonated as shown above, but becomes yellow in alkaline or basic solutions. Thus, production of the blue color of p-

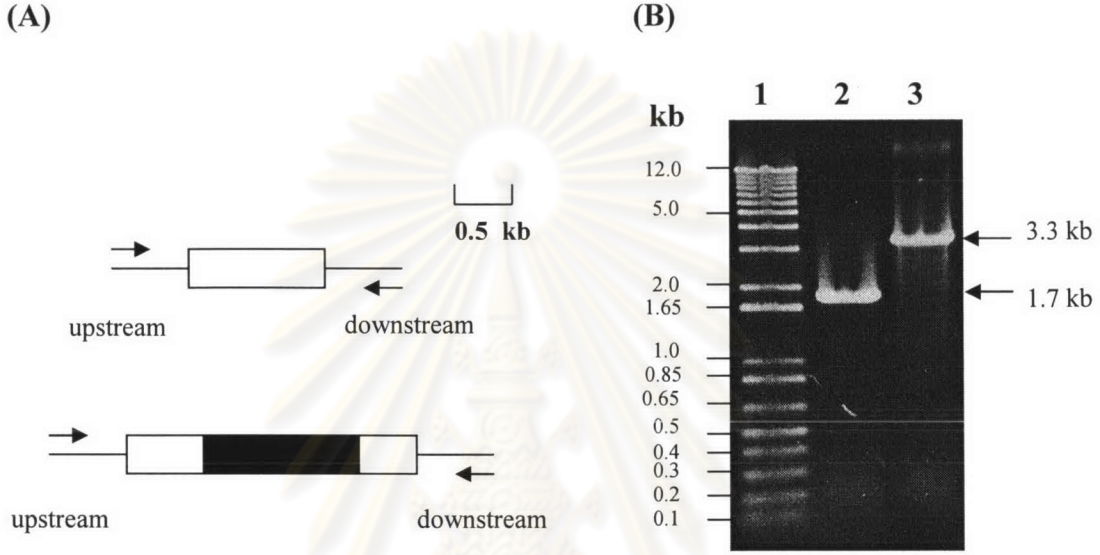

Figure 27 PCR demonstrating full segregation of the *phoU* gene interrupted with a kanamycin-resistance cassette. (A) Genomic DNA map showing the *phoU* region. The slr0741 and kanamycin-resistance cassette are shown by white and black boxes, respectively. 1 Kb Plus DNA marker (lane 1), wild type (lane 2), D88N: ΔPhoU strain (lane 3).

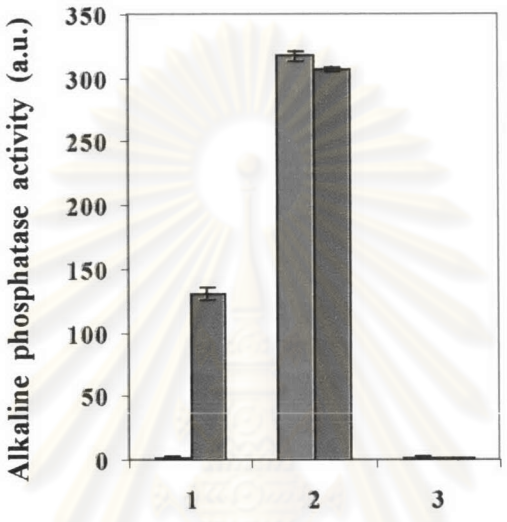

Figure 28 Measurement of alkaline phosphatase activity in the strain D88N in the absence of PhoU under phosphate-sufficient and phosphate-limiting conditions. Cells were grown in normal BG-11 (blue bars) and in phosphate-limiting BG-11 (purple bars). The strains are wild type (1); ΔPhoU (2) and D88N: ΔPhoU (3).

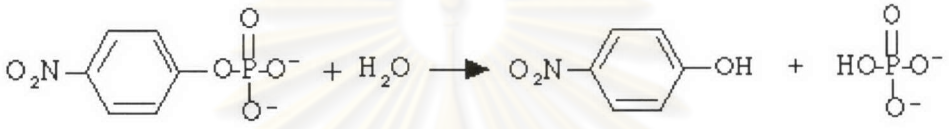

p-nitrophenyl phosphate p-nitrophenol

Figure 29 Reaction catalyzed by alkaline phosphatase.

nitrophenol in alkaline solution is measured by a spectrophotometer. In this study, the absorbance at 400 nm was used to measure the alkaline phosphatase activity in vivo. If the absorbance at 400 nm was higher than 1, the sample needed to be diluted until the absorbance was in the range of 0.2-0.8.

The ΔPhoU mutant strain was one of strains routinely giving absorbance resdings higher than 1. When the samples were diluted 5-, 8- and 10- fold, they exhibited different net absorbance depending on the dilution (Fig. 30).

After it was found that the dilution factor affects the absorbance at 400 nm, then this sample was scanned from wavelength 300-800 nm for the absorption spectrum.

From Fig. 31 the maximum absorption was found to be higher than 400 nm. The results from the measurement at the maximum absorption should be more accurate than at 400 nm. Therefore, the appropriate wavelength was investigated by measuring the absorbance of the sample at 400 nm and comparing this to reading at 405 and 420 nm.

The results of the measurement at 420 nm showed the least change when compared to these at 400 and 405 nm (Fig. 32). This indicated that the dilution factor was not so severe at 420 nm. Thus, 420 nm should be the best wavelength for alkaline phosphatase measurements.

In this study, Tris-HCl (pH 8.5) was used in the alkaline phosphatase reaction mixture. To examine effect of different buffer at the same pH, Tricine-NaOH (pH 8.5) was used instead of Tris-HCl.

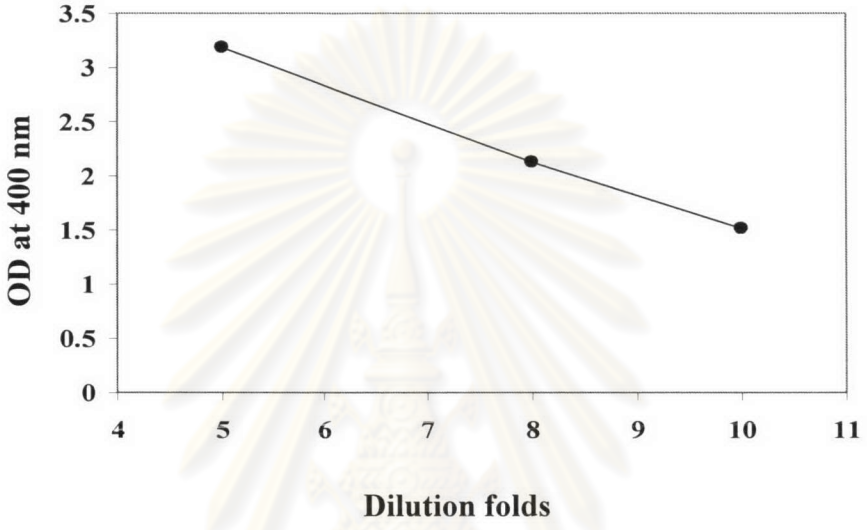

Figure 30 Effect of the dilution factor on absorbance at 400 nm of the supernatant from alkaline phosphatase reaction mixture.

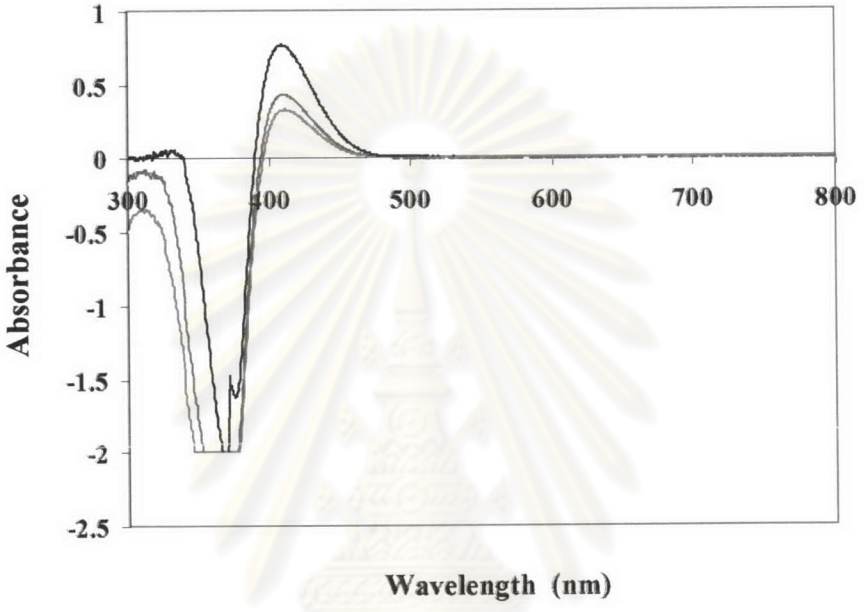

Figure 31 Absorption spectrum of the supernatant from alkaline phosphatase reaction mixture. Dilutions of 5-, 8- and 10- fold are indicated with black, green and red lines, respectively.

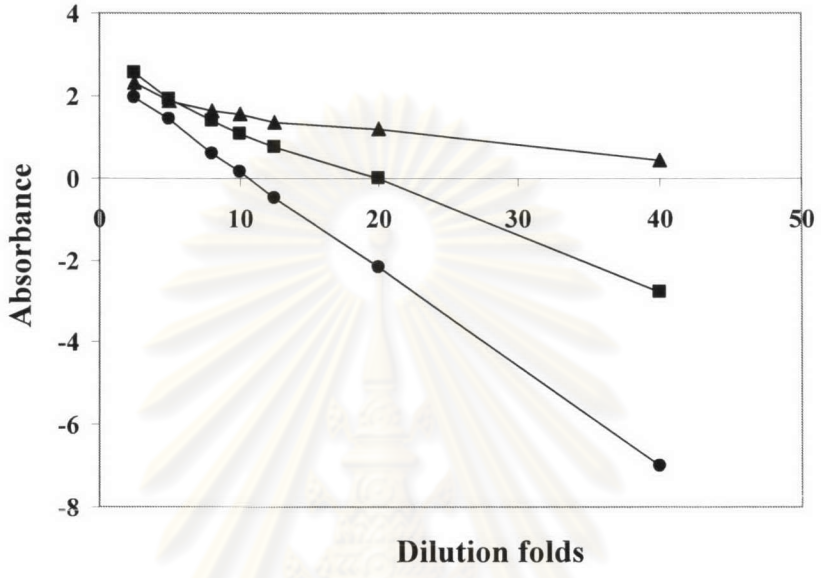

Figure 32 Dilution effect on the absorbance of the assay from the alkaline phosphatase reaction mixture at difference wavelengths. The absorbance at 400, 405 and 420 nm are shown in circles, squares and triangles, respectively.

The results from Tris-HCl and Tricine-NaOH (pH 8.5) showed the same pattern but the absorbance from Tricine-NaOH was higher than that seen in Tris-NaOH (Fig. 33). This suggested that Tris-HCl (pH 8.5) was suitable as a buffer system for the alkaline phosphatase assay.

Hence, the dilution fold and wavelength affected the alkaline phosphatase assay. Therefore the alkaline phosphatase activity of Sll0337 in the presence and absence PhoU were measured at 420 nm to ensure that the results already obtained at 400 nm were reproducible. The sample was also diluted as little as possible (Figs. 34 and 35).

The pattern of alkaline phosphatase activity obtained from the measurement at 420 nm was similar to that seen at 400 nm (Figs. 34 and 35). Therefore, the previous results with the standard deviation were from the true effect of the mutation.

3.2 Function of acetyl phosphate in Slr0081 response regulator

In *E. coli*, it has been known that PhoR can be phosphorylated by acetyl phosphate. In order to determine if the response regulator proteins can also be phosphorylated by endogenous or exogenous acetyl phosphate in absence of Sll0337, the acetate kinase encoded by *sll1299* gene was inactivated to construct a combination mutant strain of ΔSll1299/ΔSll0337. This was based on the assumption that the accumulated endogenous acetyl phosphate in this mutant may provide the chance for phosphorylation of Slr0081 by acetyl phosphate. This strain was also compared to the ΔSlr2132/ΔSll0337 and ΔSll1299/ΔSlr2132/ΔSll0337 mutants because phosphotransacetylase is encoded by slr2132 (see section 1.5). Previously, the *sll0337*

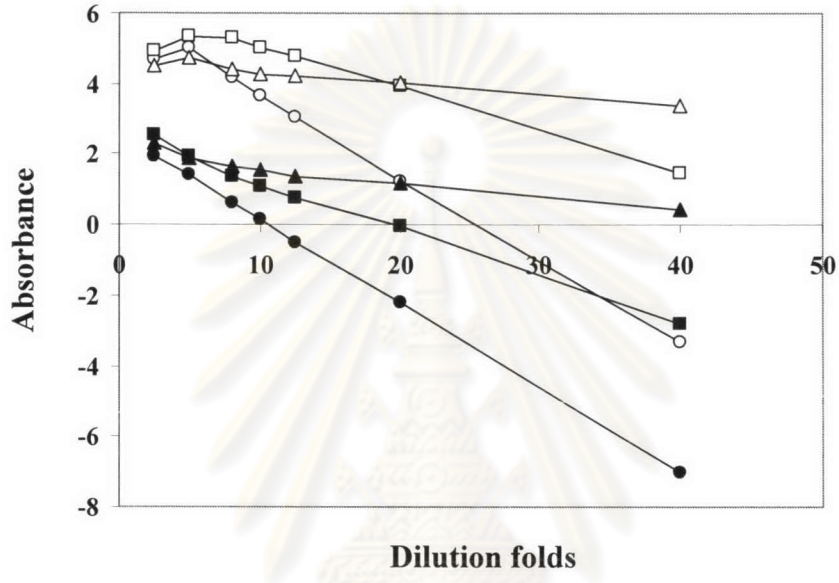

Figure 33 Dilution effect on the absorbance of the supernatant from alkaline phosphatase reaction mixture with difference buffer and wavelength. The absorbance was measured in Tricine (open symbols) and Tris (closed symbols) at 400, 405 and 420 nm as shown by circles, squares and triangles, respectively.

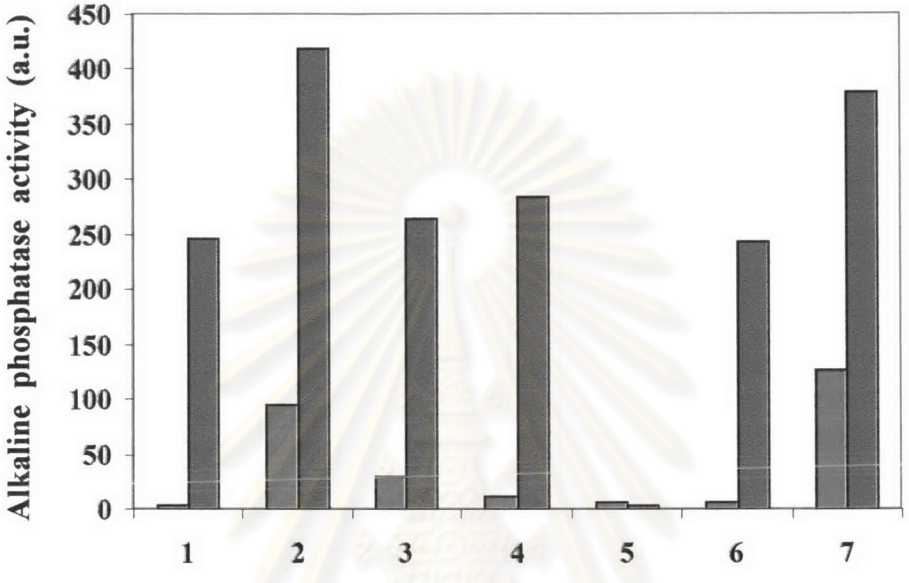

Figure 34 Measurement of alkaline phosphatase activity in strains carrying mutations at Thr-214 in Sll0337 under phosphate-sufficient and phosphate-limiting conditions. Cells were grown in normal BG-11 (blue bars) and in phosphate-limiting BG-11 (purple bars). The strains are wild type (1), T214N (2), T214S (3), T214A (4), T214R (5), T214Q (6) and T214G (7).

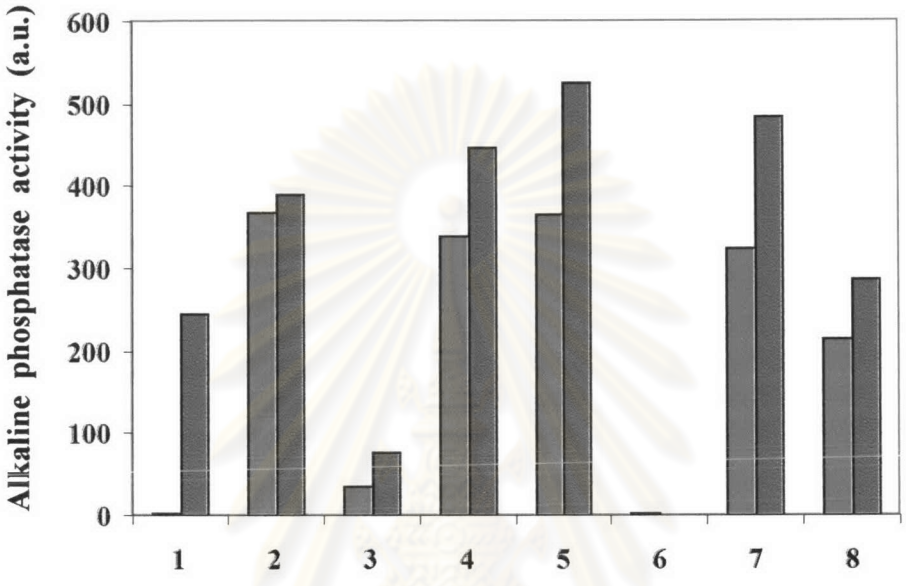

Figure 35 Measurement of alkaline phosphatase activity in strains carrying mutations at Thr-214 in the absence of PhoU under phosphate-sufficient and phosphate-limiting conditions. Cells are grown in normal BG-11 (blue bars) and in phosphate-limiting BG-11 (purple bars). The strains are wild type (1), ΔPhoU (2), T214N:ΔPhoU (3), T214S:ΔPhoU (4), T214A:ΔPhoU (5), T214R:ΔPhoU (6); T214Q:ΔPhoU (7) and T214G:ΔPhoU(8).

gene had been interrupted with a spectinomycin-resistance cassette. Therefore, the *sll1299* and *slr2132* needed to be inactivated with difference antibiotic-resistance cassettes.

3.2.1 *Construction of the sll1299 interruption plasmid*

The pUC19 plasmid containing the *sll1299* gene was interrupted with a kanamycin-resistance cassette because this selectable marker was different from that used in the sll0337 mutant. A part of the gene between two *Hpa* I site was deleted by insertion of the kanamycin-resistance cassette. Restriction enzyme digests were performed to confirm the configuration of the resulting plasmid (Fig. 36).

The *Cla* I digest was expected to linearise the plasmid, resulting in a 5.2 kb band and the *EcoR* I/*Hind* III digest yielded fragments of 2.6 kb, 1.4 kb, 0.87 kb and 0.3 kb (Fig. 36). The plasmid obtained conformed to the predicted sizes of each restriction digest thereby confirming that the pΔ*sll1299* construct with an interruption of kanamycin-resistance cassette had been constructed.

3.2.2 *Construction of the slr2132 interruption plasmid*

The pGEMT plasmid containing the *slr2132* gene was interrupted with a chloramphenicol-resistance cassette. The position of *BstE* II site was used for the insertion of the chloramphenicol-resistance cassette. Restriction enzyme digests were performed to confirm the configuration of the resulting plasmid (Fig. 37).

The *Not* I digest produced the expected three fragments 3.2 kb, 3.0 kb and 1.3 kb. The *Nco* I digest yielded a 3.4 kb, 2.3 kb, 0.9 kb and 0.85 kb as expected (Fig. 37). The plasmid obtained therefore conformed to the expected sizes of each

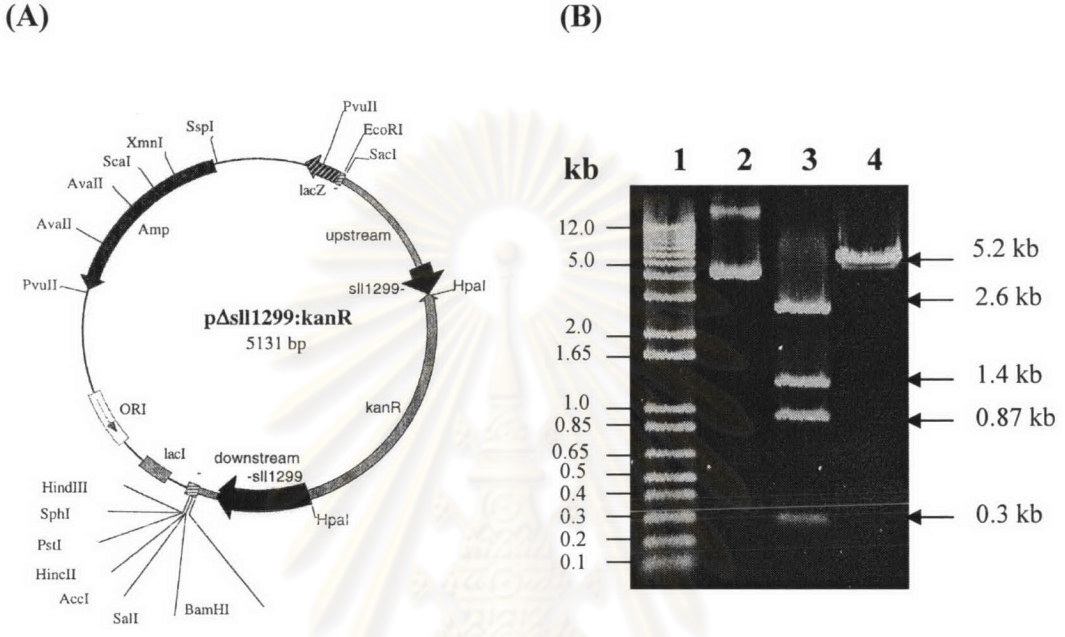

Figure 36 The pΔ*sll1299* mutant plasmid. (A) The kanamycin-resistance cassette was inserted to the p*sll1299* plasmid. The *sll1299* gene and the kanamycin-resistance cassette are showed by black and gray arrows, respectively. (B) Restriction enzyme digests of the Δ*sll1299* construct were analysed on 0.8% gel electrophoresis. 1 Kb Plus DNA marker (lane 1), uncut plasmid (lane 2), *EcoR* I/*Hind* III digest (lane 3) and *Cla* I (lane 4).

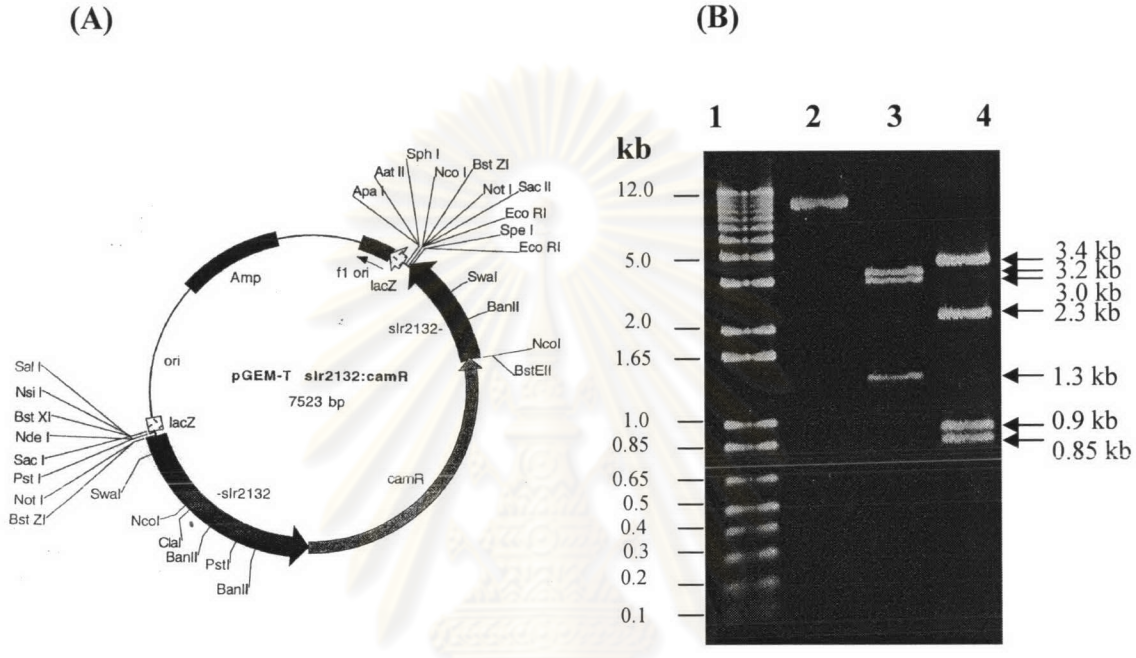

Figure 37 The pΔ*slr2132* mutant plasmid. (A) The chloramphenicol-resistance cassette is inserted to the p*slr2132* plasmid. The *slr2132* and chloramphenicol-resistance cassette are showed by black and gray arrows, respectively. (B) Restriction enzyme digests of the pΔ*slr2132* construct were analysed on 0.8% agarose gel electrophoresis. 1 Kb Plus DNA marker (lane 1), uncut plasmid (lane 2), *Not* I digest (lane 3) and *Nco* I (lane 4).

restriction digest thereby confirming that the pΔ*slr2132* construct containing an interruption by a chloramphenicol-resistance cassette in slr2132 had been constructed.

3.2.3 *Cross regulation of Slr0081 by acetyl phosphate*

The ΔSll1299/ΔSl0337, ΔSlr2132/ΔSll0337 and ΔSll1299/ΔSlr2132/ΔSll0337 mutants were constructed by transforming pΔsll1299 and/or pΔslr2132 to the ΔSll0337 mutant and wild type strain. The homozygosity of these strains was then verified by PCR using the *sll1299* and/or *slr2132* forward and reverse primers. The PCR reaction to amplify *sll1299* involved an initial denaturation at 95°C for 4 min followed by 30 cycles consisting of 1 min annealing at 69°C, 3 min extension at 72°C and 30 s denaturing at 94°C. The reaction was ended with a final extension at 72°C for 5 min. The PCR reaction to amplify *slr2132* involved an initial denaturation at 95°C for 4 min followed by 30 cycles consisting of 1 min annealing at 50°C, 4 min extension at 68°C and 30 s denaturing at 94°C. The reaction was ended with a final extension at 72°C for 5 min.

There was only a single band of 2.6 kb and 4.6 kb in the ΔSll1299/ΔSll0337 strain (Fig. 38) and ΔSlr2132/ΔSll0337 strain (Fig. 39), respectively. The ΔSll1299/ ΔSlr2132/ΔSll0337 strain showed 2.6 kb and 4.6 kb using *sll1299* and *slr2132* primers, respectively (Fig. 40) while the wild type produced 2.0 kb and 2.4 kb PCR products using sll1299 and slr2132 primers. These PCR products in each lane showed the difference in size from wild type (Figs. 38-40). Therefore segregation had been successful. Then the alkaline phosphatase activity was measured and compared to wild type.

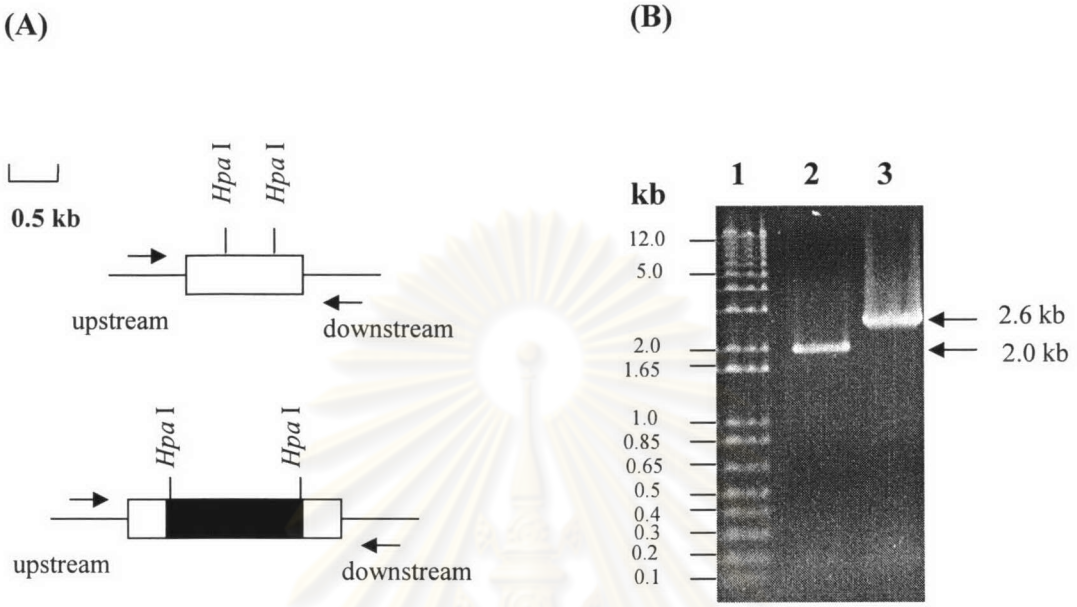

Figure 38 PCR demonstrating full segregation of the interrupted sll1299 genes containing antibiotic-resistance cassettes. (A) Genomic DNA map showing the sll1299 gene region in wild type and the sll1299:kan^R strain. The *sll1299* gene and kanamycin-resistance cassette are shown by white and back boxes, respectively. The kanamycin-resistance cassette was inserted between *Hpa* I site. The sll1299 forward and reverse primers are shown by arrows. (B) PCR products were analysed on 0.8% agarose gel electrophoresis. 1 Kb Plus DNA marker (lane 1), wild type (lane 2) and ΔSll1299/ΔSl0337 (lane 3).

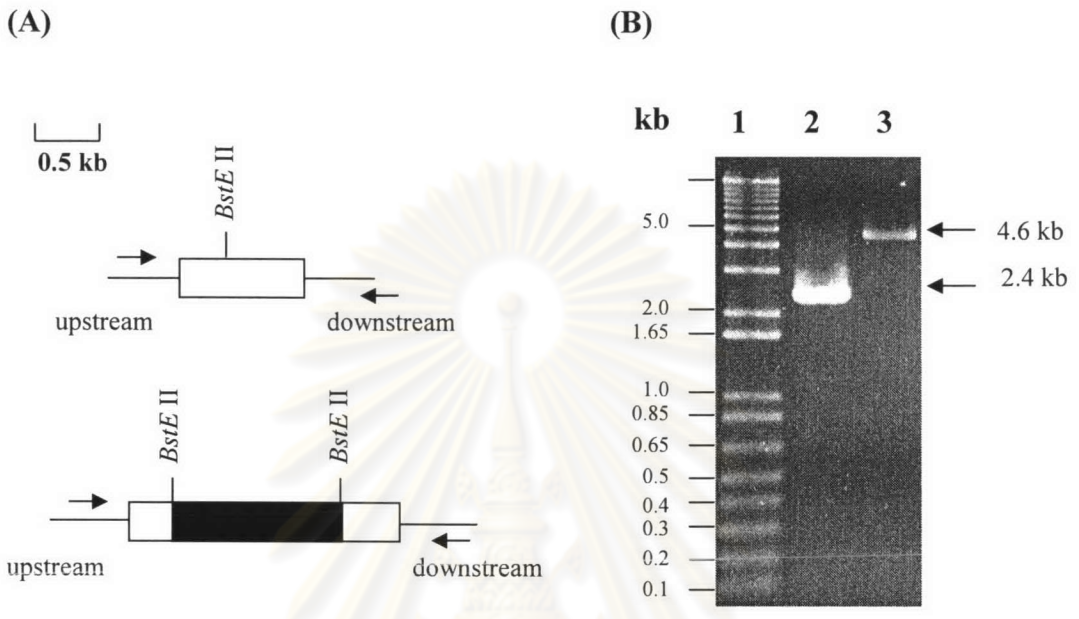

Figure 39 PCR demonstrating full segregation of the interrupted slr2132 genes containing antibiotic-resistance cassettes. (A) Genomic DNA map showing the slr2132 gene region in wild type and the slr2132:cam^R strain. The chloramphenicol-resistance cassette was inserted at *BstE* II site The *slr2132* gene and chloramphenicol-resistance cassette are shown by white and back boxes, respectively. The slr2132 forward and reverse primers are shown by arrows. (B) PCR products were analysed on 0.8% agarose gel electrophoresis. 1 Kb Plus DNA marker (lane 1), wild type (lane 2) and ΔSlr2132/ΔSl0337 (lane 3).

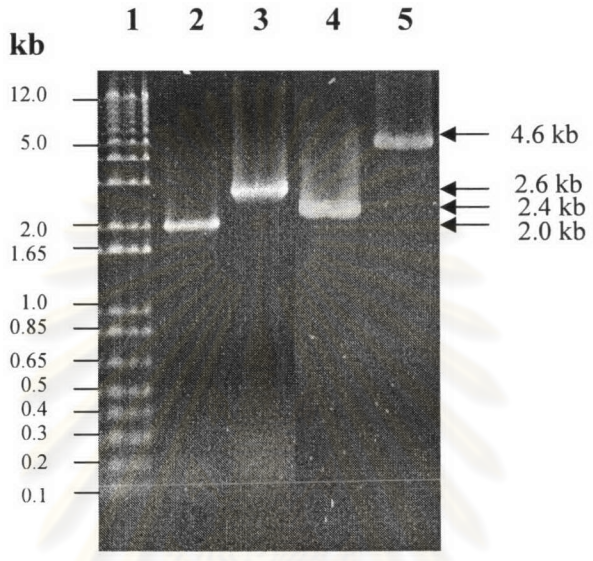

Figure 40 PCR demonstrating full segregation of the interrupted genes containing antibiotic-resistance cassettes. PCR products were analysed on 0.8% agarose gel electrophoresis. 1 Kb Plus DNA marker (lane 1), wild type using sll1299 primers (lane 2), ΔSll1299/ΔSlr2132/ΔSl0337 using sll1299 primers (lane 3), wild type using slr2132 primers (lane 4) and ΔSll1299/ΔSlr2132/ΔSl0337 using slr2132 primers

The result from Fig. 41 shows that the induction of alkaline phosphatase activity was observed in wild type grown in phosphate-limiting BG-11 (Fig. 41, lane 1). However, there was no induction of alkaline phosphatase of the ΔSll1299/ΔSl0337, ΔSlr2132/ΔSll0337 and ΔSll1299/ΔSlr2132/ΔSll0337 mutants even in phosphate-limiting BG-11(Fig. 41, lane 2-4). The results suggested that the endogenous acetyl phosphate cannot phosphorylate Slr0081 in absence of Sll0337.

3.2.4 *Acetyl phosphate as a phosphate source of the Synechocystis* sp. PCC 6803

From a previous study, the addition of acetyl phosphate restores endogenous levels of ATP in the *Synechocystis* cells under phosphate-limiting BG-11 (Hirani et al., 2001). The ΔSll1299/ΔSlr2132/ΔSll0337 strain was also used to investigate the involvement of acetate kinase and phosphotransacetylase in supplying the energy for the cells by providing a source of phosphate from exogenous acetyl phosphate.

The ΔSll1299/ΔSlr2132/ΔSll0337 mutant was grown photoautotrophically under normal and phosphate-limiting BG-11 for 7 days. The mutant cells were collected and growth was continued at $OD_{730\ nm}$ of 0.05 under normal, phosphate-limiting BG-11 and phosphate-limiting BG-11 containing 20 μM acetyl phosphate for another 7 days.

The first 7 days growth of wild type and the ΔSll1299/ΔSlr2132/ΔSll0337 mutant was retarded in phosphate-limiting BG-11 (Fig. 42A). Cells at day 7 were collected and used to start a new photoautotrophic growth curve for another 7 days. The wild type and the ΔSll1299/ΔSlr2132/ΔSll0337 strain could not grow under

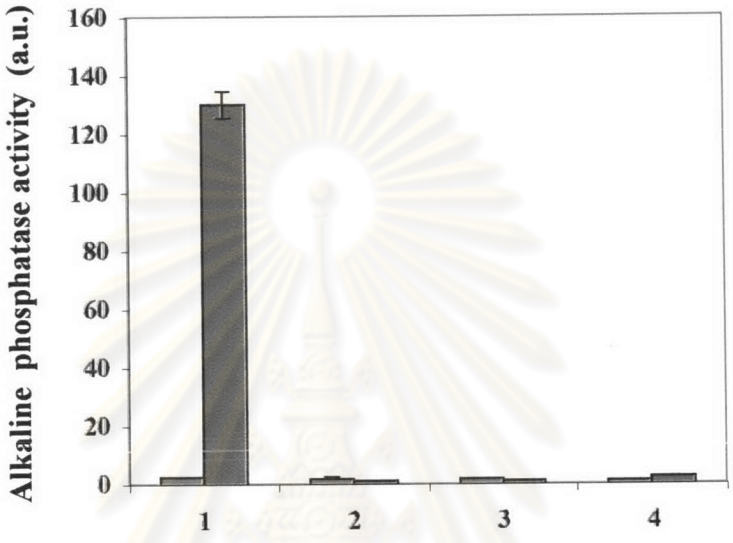

Figure 41 Measurement of alkaline phosphatase activity in ΔSll1299/ΔSll0337 under phosphate-sufficient and phosphate-limiting conditions. Cells were grown in normal BG-11 (blue bars) and in phosphate-limiting BG-11 (purple bars). The strains are wild type (1), ΔSll1299/ΔSll0337 (2), ΔSlr2132/ΔSll0337 (3) and ΔSll1299/ΔSlr2132/ Δ Sll0337 (4). The data represent Mean ± SD, n=3.

phosphate-limiting BG-11 (Fig. 42B) presumably because cells had depleted all lacked phosphate reserves. However, these strains, under the phosphate-limiting BG-11 containing 20 μM acetyl phosphate, showed similar growth to that under normal BG-11 (Fig. 42B). This result suggested that exogenous acetyl phosphate can provide phosphate for the cells even though acetate kinase and phosphotransacetylase were not present in the ΔSll1299/ΔSlr2132/ΔSll0337 mutant.

3.3 Acetate kinase and phosphotransacetylase genes are up-regulated under phosphate stress

The acetate kinase and phosphotransacetylase of *Synechocystis* sp. PCC 6803 are encoded by *sll1299* (*ack*) and *slr2132* (*pta*), respectively. To identify the mRNA expression of acetate kinase and phosphotransacetylase, RT-PCR was performed. The total RNA was extracted from wild type *Synechocystis* sp. PCC 6803 grown under normal BG-11 and phosphate-limiting BG-11 conditions. The RT-PCR was done by using a specific primer (sll1299 and slr2132 primer) to produce cDNA of the sll1299 and slr2132 genes. The cDNA of *psbB* was also produced using *psbB* primers to use as a control for the constitutive mRNA levels in both conditions. The PCR reaction to amplify *sll1299*, *slr2132* and *psbB* cDNA involved an initial denaturation at 95°C for 4 min followed by 30 cycles consisting of 1 min annealing at 59°C, 1 min extension at 72°C and 30 s denaturing at 94°C. The reaction was ended with a final extension at 72°C for 5 min.

From Fig. 43 the PCR product of the 0.52 kb band of *psbB* under normal and phosphate-limiting conditions are at the same level (Fig. 43A and B, lane 1 and

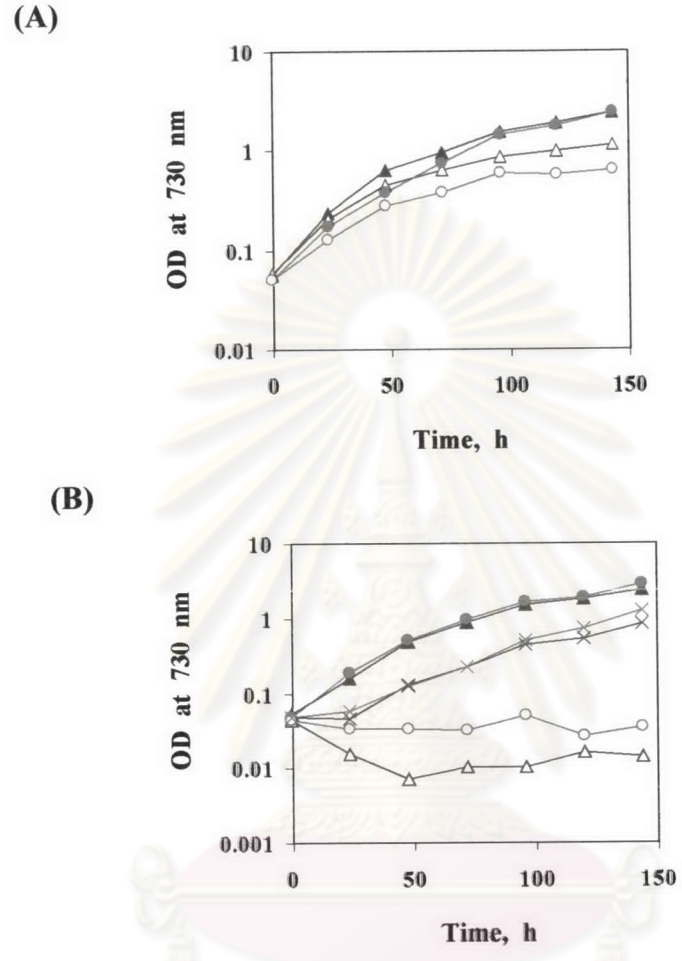

Figure 42 Photoautotrophic growth of wild type and ΔSll1299/ΔSlr2132/ΔSll0337 mutant. (A) First phase (B) Second phase of photoautotrophic growth of strains as measured by the optical density at 730 nm in normal BG-11 (closed symbols), in phosphate-limiting BG-11 (open symbols) and in phosphate-limiting BG-11 containing 20 μM acetyl phosphate(cross symbols). Wild type (red), ΔSll1299/Δ Slr2132/ΔSll0337 strain (blue).

lane 3). These bands were used for the internal control to ascertain that the difference in levels of the PCR product corresponding to acetate kinase and phosphotransacetylase was due to the difference in mRNA expression. The expected sizes of the acetate kinase gene, 0.48 kb (Fig. 43A, lane 1 and 3) and of the phosphotransacetylase gene, 0.63 kb (Fig. 43B, lane 1 and lane 3) were obtained. The results of the negative control experiment (Fig. 43A and B, lane 2 and lane 4) showed that there was no DNA in the RNA sample in the RT-PCR reaction. The levels of the PCR products of both genes are higher under phosphate-limiting BG-11 than under normal BG-11. The results show that the regulation of phosphotransacetylase and acetate kinase synthesis occur at least in part at mRNA level mediated by phosphate stress.

3.4 Purification of acetate kinase and its properties

The crude acetate kinase enzyme from *Synechocystis* sp. PCC 6803 was partially purified by 30% ammonium sulfate precipitation and then the supernatant containing 30% ammonium sulfate was loaded onto a phenyl-sepharose column. The fractions containing acetate kinase activity were eluted at ammonium sulfate concentrations between 0.2-0 M (Fig. 44). These fractions were pooled and analyzed by SDS-PAGE. The subunit molecular weight of acetate kinase from *Synechocystis* sp. PCC 6803 was found to be 48 kDa (Fig. 45). The acetate kinase activity stain was also done to follow the acetate kinase activity in each purification step (Fig. 46).

The partially purified acetate kinase was studied for its properties. Figure 47 shows that the optimum temperature for acetate kinase activity occurred at 40°C. At

the higher and lower temperature, the enzyme showed a decrease in activity. The acetate kinase can catalyse the reaction across the range pH of 6.5-8.5 (Fig. 48). The effect of the Mg^{2+} concentration on the acetate kinase activity was also performed. The results indicate that the optimum Mg^{2+}/ATP ratio is 1.0 (Fig. 49). Apparent K_m values as determined by Lineweaver-Burk plot for the substrates acetate and ATP were found to be 20 mM and 0.7 mM, respectively (Fig. 50 and 51). The substrate specificity of acetate kinase showed that the acetate kinase preferred ATP and acetate as the substrate (Table 7).

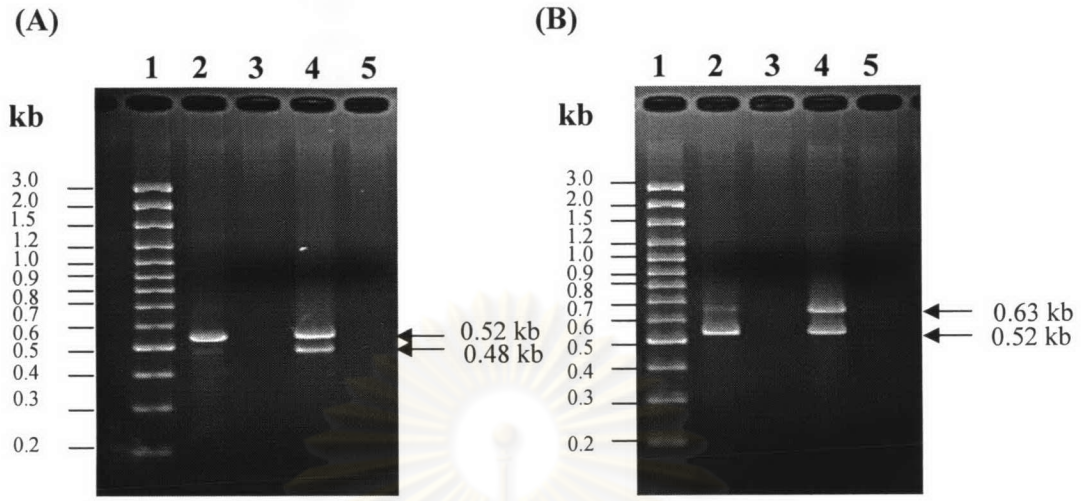

Figure 43 RT-PCR analysis of the *ack* gene and *pta* gene expression in *Synechocystis* sp. PCC 6803. (A) Transcripts of *ack* under normal and phosphate-limiting BG-11. PCR products were analysed on 2% agarose gel electrophoresis. 1 Kb Plus DNA marker (lane 1), transcript of *ack* and *psbB* genes under normal BG-11 (lane 2), negative control in which no reverse transcriptase was added to the RNA sample under normal BG-11 (lane 3), transcript of *ack* and *psbB* genes under phosphate-limiting BG-11 (lane 4) and negative control in which no reverse transcriptase was added to the RNA sample under phosphate-limiting conditions (lane 5). (B) Transcripts of *pta* under normal and phosphate-limiting BG-11. PCR products were analysed on 2% agarose gel electrophoresis. 1 Kb Plus DNA marker (lane 1), transcript of *pta* and *psbB* genes under normal BG-11 (lane 2), negative control in which no reverse transcriptase was added to the RNA sample under normal BG-11 (lane 3), transcript of *pta* and *psbB* genes under phosphate-limiting BG-11 (lane 4) and negative control in which no reverse transcriptase was added to the RNA sample under phosphate-limiting conditions (lane 5)

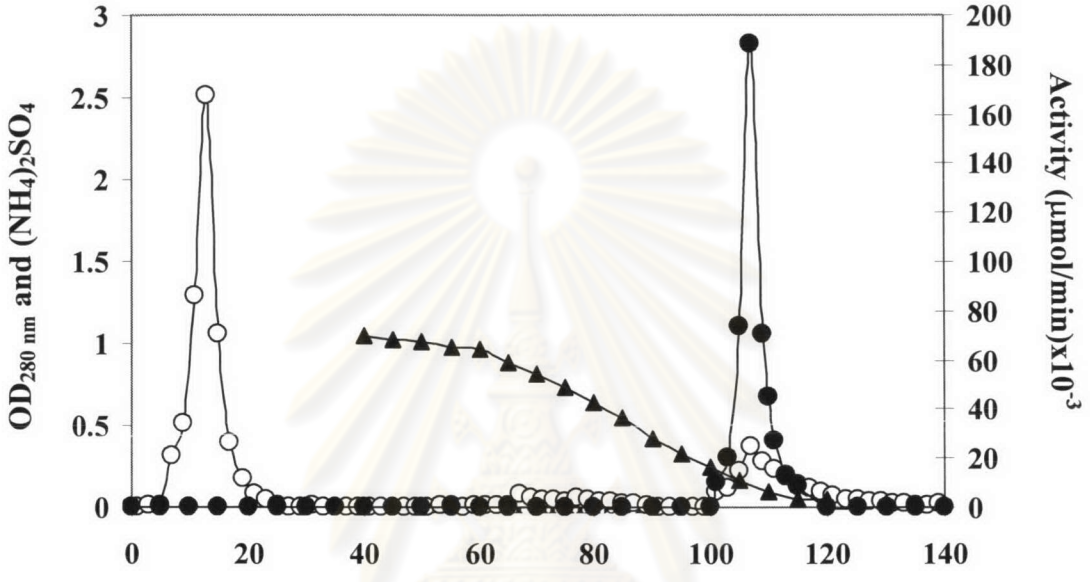

Figure 44 Phenyl-sepharose chromatography of *Synechocystis* sp. PCC 6803 acetate kinase. $OD_{280\ nm,}$ acetate kinase activity and $(NH_4)_2SO_4$ are indicated by open circles, closed circles and triangles, respectively.

Purification step	Protein (mg)	Activity (μmol/min)	Specific activity (μmol/min/mg protein)	Purification (fold)	Yield (%)
Crude	57.88	23.47	0.402	1	100
30% ammomiun sulfate	42.19	20.83	0.482	1.198	86.62
Phenyl- sepharose	6.011	15.21	2.486	6.18	64.81

Table 7 Purification of acetate kinase from *Synechocystis* sp. PCC 6803

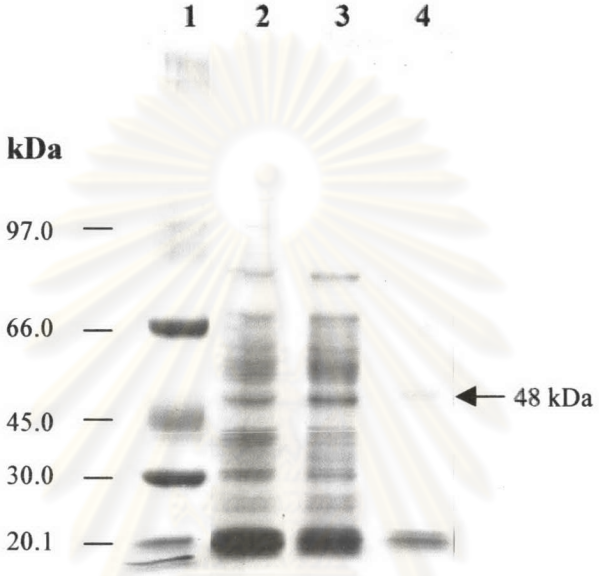

Figure 45 Acetate kinase from *Synechocystis* sp. PCC 6803 was analyzed by SDS-PAGE. Low molecular weight marker (lane 1), crude enzyme (lane 2), 30% ammonium sulfate precipitation (lane 3) and pool fractions from phenyl-sepharose (lane 4).

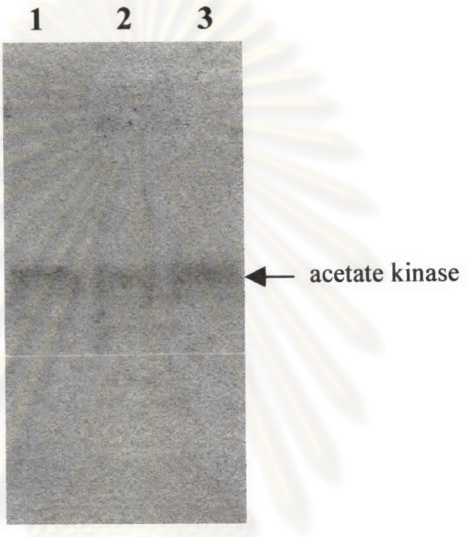

Figure 46 Acetate kinase activity stain. Crude enzyme (lane 1), 30% ammonium sulfate precipitation (lane 2) and pool fractions from phenyl-sepharose (lane 3).

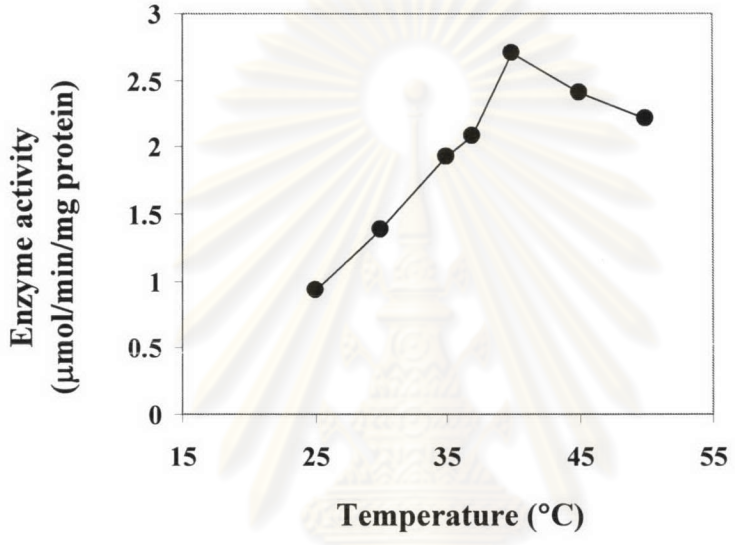

Figure 47 Effect of temperature on acetate kinase activity.

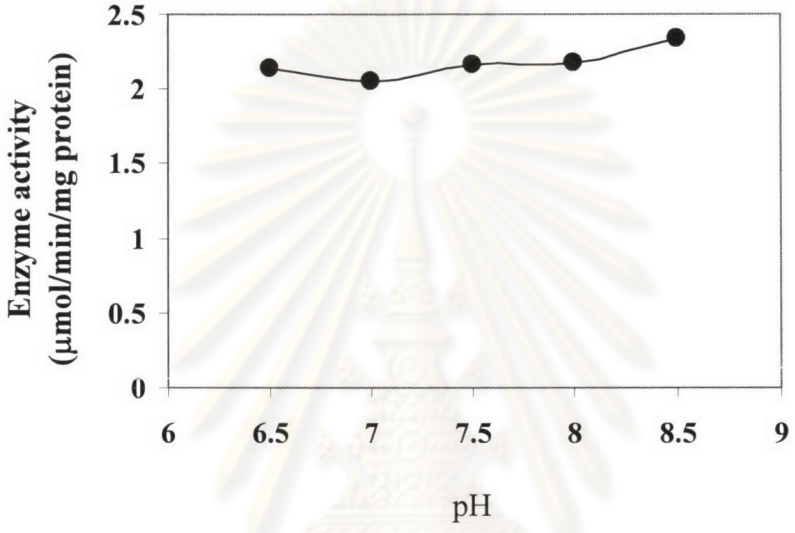

Figure 48 Effect of pH on acetate kinase activity. Acetate kinase was determined at 37°C in the following buffers: HEPES (pH 6.5 –7.5) and Tris (pH8.0-8.5).

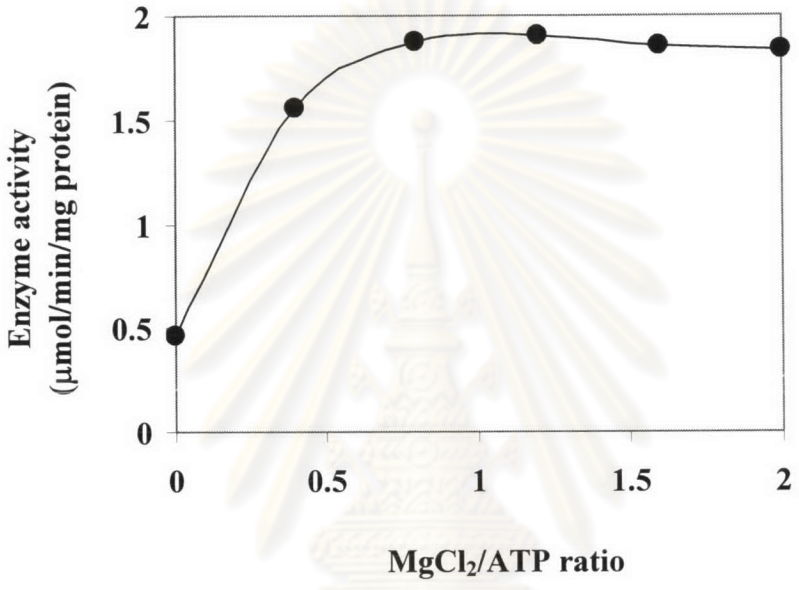

Figure 49 Effect of the Mg^{2+} concentration on the activity of acetate kinase.

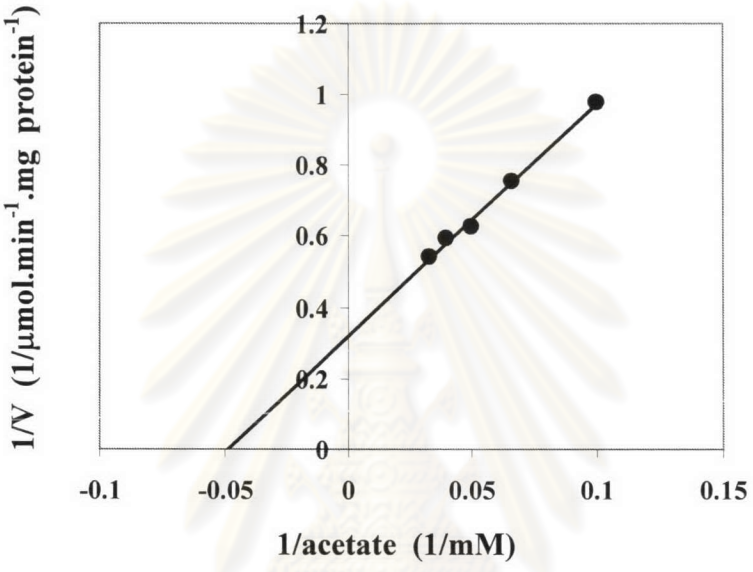

Figure 50 Double reciprocal plot of activity of partially purified acetate kinase as a function of the concentration of the substrate, acetate.

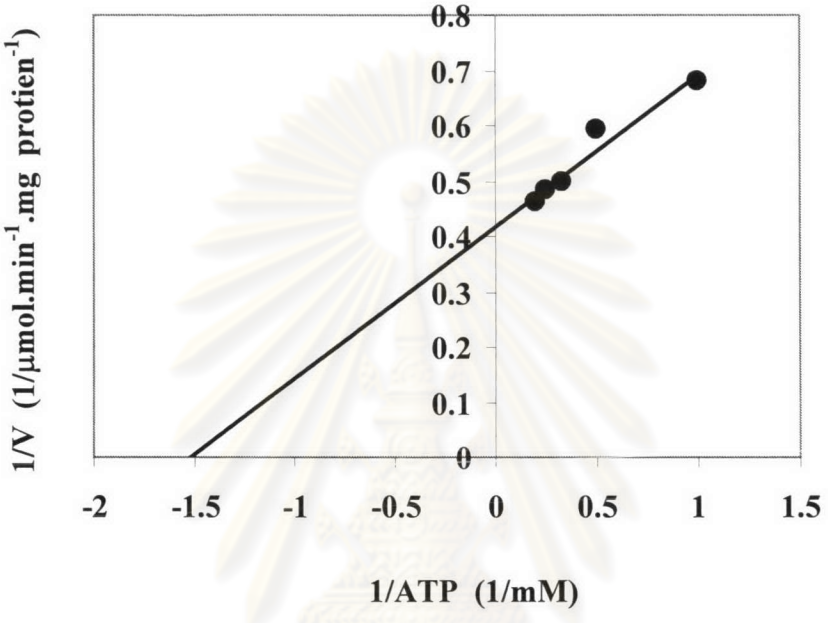

Figure 51 Double reciprocal plot of activity of partially purified acetate kinase as a function of the concentration of the substrate, ATP.

Table 8 Substrate specificity of the acetate kinase

Substrate	Concentration (mM)	Activity (%)
Acetate	50	100
Propionate	50	16
Butyrate	50	4
ATP	5	100
UTP	5	18
CTP	5	18
GTP	5	34
TTP	5	43